Regulation of coronary venular barrier function by blood borne inflammatory mediators and pharmacological tools: insights from novel microvascular wall models

Gerd Juchem, Dominik R. Weiss, Maria Knott, Anton Senftl, Stefan Förch, Theodor Fischlein, Eckart Kreuzer, Bruno Reichart, Stefan Laufer, Stephan Nees

Angaben zur Veröffentlichung / Publication details:

Juchem, Gerd, Dominik R. Weiss, Maria Knott, Anton Senftl, Stefan Förch, Theodor Fischlein, Eckart Kreuzer, Bruno Reichart, Stefan Laufer, and Stephan Nees. 2012. "Regulation of coronary venular barrier function by blood borne inflammatory mediators and pharmacological tools: insights from novel microvascular wall models." *American Journal of Physiology-Heart and Circulatory Physiology* 302 (3): H567–81. https://doi.org/10.1152/ajpheart.00360.2011.

Am J Physiol Heart Circ Physiol 302: H567–H581, 2012.
First published November 11, 2011; doi:10.1152/ajpheart.00360.2011.

Regulation of coronary venular barrier function by blood borne inflammatory mediators and pharmacological tools: insights from novel microvascular wall models

Gerd Juchem,[1]* Dominik R. Weiss,[2]* Maria Knott,[3] Anton Senftl,[3] Stefan Förch,[3] Theodor Fischlein,[4] Eckart Kreuzer,[1] Bruno Reichart,[1] Stefan Laufer,[5] and Stephan Nees[3]

[1]*Department of Cardiac Surgery, University of Munich (Ludwig Maximilians University), Munich;* [2]*Department of Transfusion Medicine and Hemostaseology, University of Erlangen-Nuremberg (Friedrich Alexander University), Erlangen;* [3]*Department of Physiology, University of Munich (Ludwig Maximilians University), Munich;* [4]*Department of Cardiac Surgery, Hospital Nuremberg South, Nuremberg; and* [5]*Department of Pharmaceutical Chemistry, University of Tuebingen (Eberhard Karls University), Munich, Germany*

Submitted 11 April 2011; accepted in final form 10 November 2011

Juchem G, Weiss DR, Knott M, Senftl A, Förch S, Fischlein T, Kreuzer E, Reichart B, Laufer S, Nees S. Regulation of coronary venular barrier function by blood borne inflammatory mediators and pharmacological tools: insights from novel microvascular wall models. *Am J Physiol Heart Circ Physiol* 302: H567–H581, 2012. First published November 11, 2011; doi:10.1152/ajpheart.00360.2011.—We hypothesized that postcapillary venules play a central role in the control of the tightness of the coronary system as a whole, particularly under inflammatory conditions. Sandwich cultures of endothelial cells and pericytes of precapillary arteriolar or postcapillary venular origin from human myocardium as models of the respective vascular walls (sandwich cultures of precapillary arteriolar or postcapillary venular origin) were exposed to thrombin and components of the acutely activatable inflammatory system, and their hydraulic conductivity (L_P) was registered. L_P of SC-PAO remained low under all conditions ($3.24 \pm 0.52 \cdot 10^{-8} cm \cdot s^{-1} \cdot cmH_2O^{-1}$). In contrast, in the venular wall model, PGE_2, platelet-activating factor (PAF), leukotriene B_4 (LTB_4), IL-6, and IL-8 induced a prompt, concentration-dependent, up to 10-fold increase in L_P with synergistic support when combined. PAF and LTB_4 released by metabolically cooperating platelets, and polymorphonuclear leucocytes (PMNs) caused selectively venular endothelial cells to contract and to open their clefts widely. This breakdown of the barrier function was preventable and even reversible within 6–8 h by the presence of 50 μM quercetin glucuronide (QG). LTB_4 synthesis was facilitated by biochemical involvement of erythrocytes. Platelets segregated in the arterioles and PMNs in the venules of blood-perfused human myocardium (histological studies on donor hearts refused for heart transplantation). Extrapolating these findings to the coronary microcirculation in vivo would imply that the latter's complex functionality after accumulation of blood borne inflammatory mediators can change rapidly due to selective breakdown of the postcapillary venular barrier. The resulting inflammatory edema and venulo-thrombosis will severely impair myocardial performance. The protection afforded by QG could be of particular relevance in the context of cardiosurgical intervention.

coronary microcirculation; endothelial cells; pericytes; inflammation; thrombosis; polymorphonuclear leucocytes

THE CONCEPT OF THE EXISTENCE of a morphological barrier between blood and surrounding parenchymal tissue was introduced more than 100 years ago (45) for the central nervous system. Blood organ barriers hinder free diffusion and/or convective transport of small hydrophilic substances (dyes, nutrients, and drugs) from the blood into the extravasal space or interstitial fluid and prevent the contact of the zymogens of the coagulation system and of many components of the immunological system with the parenchymal cells and tissues around the blood vessels. Classic examples in this respect are the blood brain, blood retina, and blood cerebrospinal fluid barriers (15, 37, 74), the morphological correlate of which is generally believed to be the particularly tight wall structure of the relevant capillaries, which belong to the tightest grade (A-1-β) in Bennett's traditional classification scale (10).

For the heart, the possibility of a blood-myocardium barrier has not been addressed to date, although evidence thereof has been available for some time. The capillaries of the ventricular myocardium, at least those of the arterial limb of the capillary system, clearly also are type A-1-β-terminal vessels possessing a continuous basal membrane, endothelium, and a dense pericapillary cellular investment (63, 64, 84). In contrast to the cerebral capillaries, the myocardial capillaries are not sheathed by astrocytes. However, the highly active coronary endothelial metabolism constitutes, at least for certain substances, an additional, metabolic barrier. Substances initially present in the coronary blood can be degraded rapidly at the endothelial surface (e.g., adenine nucleotides; Refs. 61, 62, 65); others are taken up rapidly by the endothelium and metabolized intracellularly, whereby they may be trapped, e.g., by phosphorylation, like adenosine (62). Whatever the mechanism, such substances, when present in the coronary lumen, do not appear extravascularly.

Studies such as those just cited (79) can also be seen in the wider context of the elucidation of endothelium-mediated vascular responsiveness. The coronary system behaves similarly to other vascular beds in that numerous naturally occurring, hydrophilic vasoactive substances, when present in the blood, function as vasodilators, thus enhancing blood flow, while the same substances when present extravasally function mostly as vasoconstrictors (e.g., paradox reaction of acetylcholine; Refs. 24, 57). This infers that there is also a barrier to diffusion in the walls of the coronary arteries and arterioles preventing the transmural passage of vasoactive substances under physiological conditions. Indeed, we (63) have shown recently that an intermediate tube, consisting of closely arranged pericytes and their hydrophobic extracellular matrix (ECM), separates the

* G. Juchem and D. R. Weiss researchers contributed equally to this work.
Address for reprint requests and other correspondence: S. Nees, Dept. of Physiology, Univ. of Munich (LMU), Schillerstr. 44, 80336 Munich, Germany (e-mail: stephan.nees@lrz.uni-muenchen.de or stephan@snees.de).

smooth muscle from the endothelium in human ventricular myocardial arteries and arterioles. This intercalated tube, which is intimately associated with the endothelial core tube, may well function as a tight barrier against the diffusion of hydrophilic substances from the coronary lumen to the vascular musculature.

In the myocardial postcapillary venules, a barrier between the blood and the myocardium also presumably exists, although the continuous endothelium of these smallest veins is not invested by a dense, but net-like ECM and pericyte layer (63, 96). In addition, venular endothelial junctions (19) are generally only loosely organized compared with those of the arteriolar endothelium (84, 85), and the venular endothelium is apparently able to contract actively and open its junctions widely (52). Should this occur, as during local inflammatory processes, rapid extravasation of plasma and hence selective recruitment of most of the humoral components of the immunological defense and hemostasiological systems into the interstitial space will result (32), in turn causing a blockade of the draining venules by fibrin thrombi and hence isolation of the affected area from the rest of the microcirculation. That the centers of inflammatory foci are not perfused is long known, and this fact can now also be explained. The key role in this circulatory "uncoupling" process is played by the subendothelial pericytes in their cocoon of ECM components, which possesses a constitutive, highly prothrombotic potency due to incorporation of abundant tissue factor and prothrombinase (14, 38, 48, 64). All these complex reactions subserve the concentration and activation of the immune defense in the vicinity of the lesion or focus of infection, thus protecting the rest of the body. Should the defense be inadequate and the inflammation spreads or generalizes, the result will be organ failure due to an insufficient microcirculation. Indeed, reports in recent years have increasingly recognized histologically demonstrable "venulo-occlusive processes" (21), "venular thrombosis" (25), or "perivenulitis" (35) as the arliest signs of organ failure or allograft rejection, e.g., rejection of transplanted hearts (72).

Against the foregoing background we developed the following working hypothesis. First, a comprehensive vascular barrier between the blood and the parenchyma of an organ will necessarily reflect the integrated barrier features of all microcirculatory segments. The presence of tight capillaries is a necessary, but alone not sufficient, prerequisite for a blood-organ barrier. Second, while the tightness of arterioles and type A-1-β capillaries depends critically on tight junctions and the pericyte cocoon, i.e., primarily on more-or-less static cell biological characteristics and physical properties, that of the venules depends on the rapidly changeable contractile state of the venular endothelium. Third, with the appearance of inflammatory mediators in the microcirculation of an organ with a normally tight barrier in all microcirculatory segments, as in the ventricular myocardium, it is the reaction of the postcapillary venular barrier that will decisively determine the clinical prognosis.

In the present study, key aspects of this working hypothesis were examined experimentally with respect to the heart using novel in vitro models of the precapillary arteriolar and postcapillary venular vessel walls derived from human ventricular myocardium (63). Activated and metabolically cooperating platelets and polymorphonuclear leucocytes (PMNs) induced breakdown of the barrier function [as reflected by the hydraulic conductivity (L_P)] only in the venular wall model. The flavonoid compound quercetin-3-*O*-β-D-glucuronide (QG) obviated this damage, even in the continued presence of the blood cells. Extrapolating these findings to the myocardial microcirculation in vivo implies strongly that the tightness and multifunctionality of the latter under numerous clinically relevant conditions can change rapidly (and threateningly) primarily due to the high degree of reactivity of the venules. The protective action of QG is of particular relevance in the context of cardiosurgical interventions and preservation of explanted organs.

MATERIALS AND METHODS

All experiments on explanted hearts and vascular cell cultures of human myocardial origin were done with written informed consent of the patients and with approval of the ethical committee of the Ludwig Maximilians University of Munich according to the principles expressed in the Declaration of Helsinki.

Materials

Polymorphoprep was supplied by Axis-Shield (Oslo, Norway); lipoxin A_4 and PGE_2 were purchased from Biomol (Hamburg, Germany); plasma substitute Biseko was supplied by Biotest (Dreieich, Germany); QG was obtained from Boehringer Ingelheim (Ingelheim, Germany); 6-[6-(3R-hydroxy-1E,5Z-undecadien-1-yl)-2-pyridinyl]-1,5S-hexanediol (U-75302) was obtained from Cayman chemical (AnnArbor, MI); Transwell polyethylenterephthalat culture supports with a surface area of 4.5 cm^2, a pore size of 0.4 μm, and a pore density of $10^8/cm^2$ were from Corning (Corning, NY); rofecoxib was commercially available from Forest Laboratories (New York, NY); Percoll was bought from GE Healthcare Europe (Freiburg, Germany); DMEM, FCS, streptomycin, penicillin, balanced salt solution (BSS), PBS, and trypsin/EDTA solution were purchased from Invitrogen (Karlsruhe, Germany); platelet-activating factor (PAF)-16-antagonist was obtained from Merck Biosciences (Bad Soden, Germany); tissue culture solution endothelial cell growth medium was supplied by Promocell (Heidelberg, Germany); adenosine deaminase, collagenase D, and dispase I were obtained from Roche Diagnostics (Mannheim, Germany); 60 U/mg trypsin were purchased from Serva (Heidelberg, Germany); Ficoll 70, Fast Blue BB, Fast Red TR, naphthol-AS-MX-phosphate, Fast Blue B, gly-Pro-4-methoxy-β-naphthylamide, acetylsalicylic acid (ASA), H_2O_2, IL-6, IL-8, PAF-16, arachidonic acid (AA), leukotriene leukotriene B_4 (LTB_4), FMLP, recombinant human complement factor C5a, human thrombin, LPS, glutaraldehyde, and OsO_4 were from Sigma (St. Louis, MO).

Histological Techniques

Tissue fixation. IMMUNOHISTOCHEMISTRY. tissue cultures were prefixed for 2 min at room temperature by immersion in 4% paraformaldehyde (PA) in PBS, stored overnight in PA at 4°C, permeabilized with 1% Triton X-100 in PBS for 30 min, and washed with PBS.

ENZYME HISTOCHEMISTRY. cell cultures were treated for 30 s with glutaraldehyde/PA and 15 min in PA followed by three washings in PBS; heart ventricles were perfused with the same fixatives for analogous periods.

Staining techniques. F-actin in endothelial cells was visualized by fluorescent phalloidin (Sigma); alkaline phosphate and dipeptidyl aminopeptidase IV activity was visualized histochemically using standard procedures (7, 100).

Time-lapse videomicroscopy. The isolation of pure postcapillary venules is described in detail elsewhere (63).

Endothelial cells and pericytes derived from such preparations were seeded in circular spots (3- to 4-mm diameter) in a 6-cm diameter Petri dish. After 2 wk, large and homogenous endothelial

colonies developed (>1 cm diameter), which were typically surrounded by pericytes (63). Such dishes were supplied with fresh culture medium and mounted within a custom-built incubator on the stage of an Axiovert 200 microscope (Zeiss, Göttingen, Germany). Time-lapse video recordings of cellular interactions on venular endothelial cell cultures were started after 1 day in complete darkness under dimmed, yellow light (maximal light absorbance ~430 nm). An automatic shutter device prevented continuous illumination of the cultures during longer (>2 h) recordings.

Preparation of Sandwich Cultures of Endothelial Cells and Pericytes of Precapillary Arteriolar and Postcapillary Venular Origin

The establishment of the sandwich cultures is described in detail elsewhere (63). In brief, the smallest arteries and veins from ventricular myocardium of human explant hearts (freshly obtained in the course of heart transplantations; their isolated tips were perfused via cannulae fixed in the main coronary arteries) were dissociated proteolytically under aseptic conditions using essentially the experimental approach described earlier (66) and our own dispersion and separation techniques (63). The microvessels were fractionated by isotonic Percoll density gradient centrifugation. Highly purified venules and arterioles were obtained at buoyant densities of 1.058 ± 0.005 and 1.050 ± 0.005 g/cm^3 respectively.

Arteriolar harvests were first cultivated for 4 days in human endothelial serum-free media basal growth medium (GIBCO/Sigma) supplemented with 10% FCS (vol/vol), 200 U/ml penicillin, 0.2 mg/ml streptomycin, 1 μg/ml fibronectin, 10 ng/ml EGF, and 20 ng/ml basic FGF. Subsequently, the cultures were incubated to confluence in a 1:1 mixture of DMEM and endothelial growth culture, which had been adjusted to 6% (vol/vol) FCS and was supplemented with penicillin and streptomycin ("mixed medium").

Cell and vessel fragments of venular origin were cultivated from the beginning until confluency in same mixed medium.

Purified colonies of venular or arteriolar endothelial origin were detached with a minimum amount of trypsin/EDTA, diluted with a 10-fold higher volume of mixed medium and seeded into Transwell inserts (~10^5 cells/cm^2), and cultivated under standard conditions (37°C, P_{CO_2} = 40 mmHg, water-saturated atmosphere). One day later, smaller numbers of pericytes (~$5 \cdot 10^3$ cells/cm$^{2)}$ were seeded on the lower surface of the polyethylenterephthalat membrane basically as described by Nakagawa et al.(60). Cultivation of these sandwich cultures proceeded for 5 days in mixed medium before the insets were inserted into the filtration apparatus (see below).

Preparation of Blood Cells and Cell-Free Supernatant

Isolation of PMNs. Aliquots (5 ml) from 50 ml freshly drawn citrated blood from healthy donors (who had refrained from taking any medication for ≥2 wk) were layered on 5 ml Polymorphoprep solution and centrifuged according to the supplier's instructions. The purified PMN bands were aspirated, combined, and diluted with BSS. After low-speed centrifugation at 800 *g*, the pellet was resuspended in a mixture of 2 ml BSS and 0.5 ml autologous citrated plasma.

Isolation of platelets. Cells from 10 ml freshly prepared platelet-rich plasma were centrifuged at 600 *g* through isotonic Percoll solution (specific density *d* 1.05 g/ml, pH 7.4) supplemented with 100 μM adenosine. Platelets concentrated in a band on top of 1 ml of isotonic Percoll solution (*d* = 1.10 g/ml), which had been underlayered before centrifugation. This band (~0.5 ml) was aspirated and diluted to a final volume of 2.5 ml with BSS supplemented with 2 IU adenosine deaminase to degrade the platelet inhibitor adenosine. Platelets (and also PMN) were used within 2 h.

Isolation of erythrocytes. These cells were purified according to Beutler et al. (11).

Preparation of standardized supernatant of activated PMN/platelets. $CaCl_2$ (2 mM), FMLP (10 μM), and ADP (100 μM) were added after mixing equal volumes of the above preparations of purified PMNs and platelets (final cell concentrations: PMN, 4,400/μl ± 10%; platelets, 70,000/μl ± 10%). The suspension was incubated at 37°C for 10 min, centrifuged at 15,000 *g* for 10 min, and filtered (sterile filter, 0.2-μm pore size). Dilutions (1:10) of this solution with basal filtration medium containing 5% Ficoll 70 (see below) were used routinely to induce a prompt massive breakdown of venular endothelial cell barriers in many of the experiments.

Measurement of L_P in the Presence of Pharmacological Inhibitors

The preparation of sandwich cultures of constituent precapillary arteriolar or postcapillary venular wall cells and the measurement of L_P of these microvascular wall models in a custom-made apparatus are described in detail elsewhere (63).

The blood cell suspensions (preparation see above), chemical solutions, or solutions with PMN/platelet release products to be brought into direct contact with the adapted endothelial barriers of Transwell cultures (4 ml in all cases) were mixed with 1 ml 25% (wt/vol) solution of Ficoll 70 in filtration medium (the latter was prepared by mixing 7 vol serum-free endothelial cell growth medium with 3 vol Biseko. Before use, this mixture was dialyzed extensively against freshly prepared human citrate plasma supplemented with 10,000 U/ml penicillin and 10 μg/ml streptomycin. Finally, the dialysate was adjusted to a concentration of free calcium ions of 4 mM, centrifuged for 1 h at 15.000 *g*, and sterilized by filtration). The above samples were then layered slowly onto the confluent endothelial sheets on their filter membranes. To inhibit cyclooxygenase-1 (COX-1) activity in endothelial cells, a 500-μM ASA solution was overlayered on endothelial barriers for 30 min and then filtered through the cell layer. COX-1 in platelets was inactivated by addition of 500 μM ASA for 30 min to the suspensions, the latter were either brought in contact with endothelial barriers directly or after transfer of platelets in ASA-free BSS. To inhibit COX-2 activity in endothelial barriers, the latter were preincubated with 50 μM rofecoxib for 30 min. To inhibit 5-lipoxygenase (5-LOX) activity, PMNs were preincubated with 50 μM {[3-fluoro-5-(4-methoxy-3,4,5,6-tetrahydro-2H-pyran-4-yl)]phenoxymethyl}-1-methyl-2-quinolone (ZD2138) or [4-(quinolin-2-ylmethoxy)-phenyl]-cycloheptyl-acetic acid (BAY-X-1007) and then cocultured with endothelial sheets. To inhibit the effect of LTB_4, U-75302 (an LTB_4 receptor antagonist) was added to the filtration medium. For eicosanoid generation and release experiments in Petri dishes (Falcon 3001), ~10^6 confluent venular endothelial cells [upper layer of sandwich culture of postcapillary venular origin (SC-PVO)] were preincubated for 4 h in 1 + 10 diluted standardized supernatant of activated PMNs/platelets in modified Krebs-Henseleit medium, washed, and incubated with 10^6 PMNs for 60 min in the presence of 20 μM AA and 100 nM PAF-16, either in the absence or presence of various eicosanoid inhibitors in 1 ml modified Krebs-Henseleit medium.

Transendothelial flow was measured continuously using a sensitive electronic balance (Sartorius, Göttingen, Germany; type: ultramicro-ME) and recorded online. After an initiation phase of 10 min, measured flow rates under all conditions tested were constant for ≥20 min and proportional to the concentration of inflammatory mediators in the filtration medium.

Synthesis of Various Pharmacological Inhibitors by Sui Laboris

ZD2138 (a 5-LOX inhibitor; CAS no. 140841-32-3) was synthesized according to the ICI Patent 0385662 (1990), and rofecoxib (a COX-2 inhibitor; CAS no. 162011-90-7) according to Merck Frosst Canada, Patent WO 9608482. BAY-X-1007 (FLAP, a 5-LOX-activating protein inhibitor) was synthesized with slight variations according to a method derived from patent DE3900261A1. In brief, after protection of the hydroxy function of 4-hydroxyphenyl acetic acid methyl ester by reaction with benzyl chloride, the methylene group of the intermediate was alkylated by cycloheptyl bromide, yielding

(4-benzyloxy-phenyl)cycloheptyl acetic acid methyl ester. After hydrogenolytic removal of the protecting group, the hydroxy group was esterified by 2-chloromethyl quinoline hydrochloride, forming [4-(quinolin-2-yl-methoxy)-phenyl]-cycloheptyl acetic acid methyl ester. The final step was cleavage of the ester to give the free acid, [4-(quinolin-2-yl-methoxy)-phenyl]-cycloheptyl acetic acid. Since the intermediate products could not be isolated as precipitates after addition of water, they were isolated by extraction with ethyl acetate after adjusting the pH to 5.5.

Assay of LTB_4, PGE_2, and PGI_2

These assays were carried out in duplicate in coculture supernatants using commercially available ELISA kits (Cayman Chemical, Milan, Italy) following the manufacturer's instructions.

Histological Demonstration of Platelets and PMNs in the Microvasculature of Isolated Perfused Human Heart Tips

Prewarmed human heart tips (from surgically rejected hearts of donors of known blood group) prepared as described elsewhere (63) were perfused for 30 min with Krebs-Henseleit medium and then circumfused with 100 ml of the commercially available plasma substitute "Biseko" for 30 min at 37°C. This protocol was repeated with a fresh batch of 100 ml Biseko for another 30 min. Thereafter, 10 ml of standardized supernatant of activated PMNs/platelets were diluted with 100 ml Biseko and circumfused for 10 min. Following subsequent admixture of 110 ml group-matched heparinized whole blood and addition of ADP (100 μM) and FMLP (1 μM) to activate platelets and PMNs, circumfusion was continued for further 30 min. Thereafter, a concentrated solution of Evans blue in 25 mM HEPES-buffered Earle's salt solution without calcium was added to the reservoir until the perfusate turned intensively blue, and the procedure was continued for another 2 min so as to demarcate the perfused myocardial areas. Subsequently, these were dissected, immediately cut into small cubes (~100 mm^3), and frozen in liquid nitrogen. All enzymatic histochemical stainings were performed in 40-μm-thick cryopreserved sections, which were postfixed for 5 min. Platelets were primary labeled with monoclonal (BL-E6) anti-CD 61 (Sigma) and PMNs with monoclonal (BM-2) anti-PMN (MBL, Nagoya, Japan). Immunological staining was performed using alkaline phosphatase-linked anti-mouse IgG antibody and azo dye coupling components Fast Blue BB (blue dye) or Fast Red TR (brick red).

Statistical Analysis

Data are presented as means ± SD. Comparisons of group data were performed using a one-way ANOVA followed by the Student-Newman-Keuls post hoc test. $P < 0.05$ was considered significant.

RESULTS

Influence of Various Activated Blood Components on the L_P of Microvascular Wall Models

Basic experiments on sandwich cultures of precapillary arteriolar (SC-PAO) or SC-PVO showed that the L_p of SC-PVO is determined mainly by the confluent endothelial tissue; a physical influence of their wide-meshed cellular net of pericytes on the hydrodynamic resistance was insignificant (63). In contrast, in the arteriolar wall model the pericyte layer contributed substantially to the tightness (and correspondingly low L_P), very probably via the organization of a continuous ECM along their entire basal surface, which opposed the coordinated endothelial sheet.

Figure 1, *lane a*, shows that model vessel walls of precapillary arteriolar origin (SC-PAO) are indeed much "tighter" (lower L_P) than those cultured from postcapillary venules (SC-PVO) of the same hearts under basal conditions (L_P of SC-PAO: $3.24 \pm 0.52 \cdot 10^{-8} cm \cdot s^{-1} \cdot cmH_2O^{-1}$, $n = 37$; basal L_P of SC-PVO: $2.55 \pm 0.32 \cdot 10^{-7} cm \cdot s^{-1} \cdot cmH_2O^{-1}$, $n = 8$).

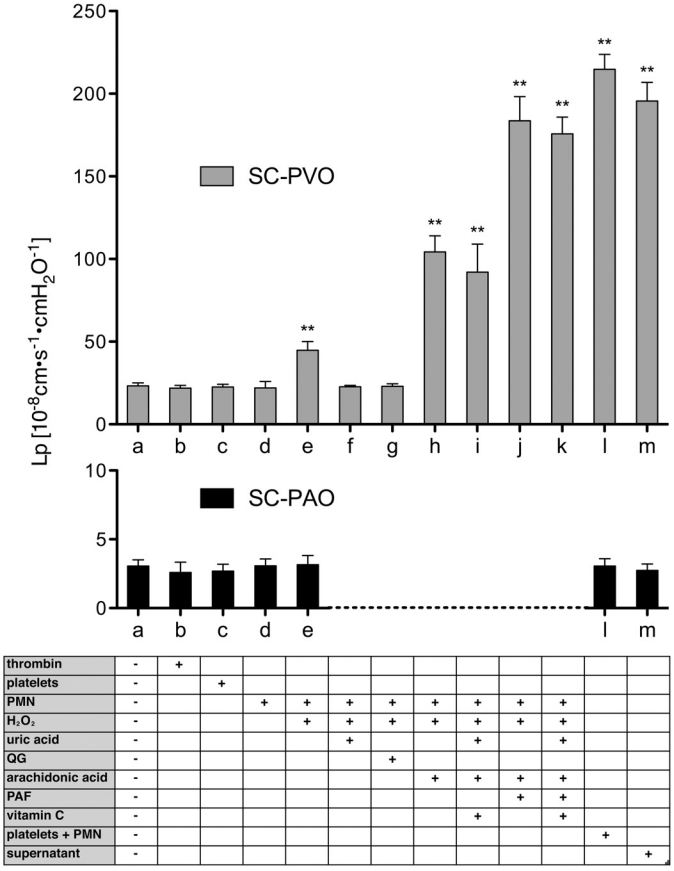

Fig. 1. In vitro sandwich culture models of the human postcapillary venular (SC-PVO) or precapillary arteriolar vessel wall (SC-PAO) react differently to exposure to activated blood components. Measurements were started in the absence or presence of various additives (scheme in the table at *bottom*) and performed over 30-min intervals at 37°C. *Lane a*: filtration medium (basal conditions); *lane b*: thrombin (1 IU/ml); *lane c*: ADP (100 μM)-activated platelets (100 platelets/1 venular or arteriolar endothelial cells); *lane d*: FMLP (1 μM)-activated polymorphonuclear leucocytes (PMNs) (10 PMN/1 venular or arteriolar endothelial cell); *lane e*: as in *lane d* + 10 μM H_2O_2; *lane f*: as in *lane e* + 100 μM uric acid; *lane g*: as in *lane e* + 100 μM quercetin glucuronide (QG); *lane h*: as in *lane e* + 100 nM arachidonic acid (AA); lane *i*: as in *lane h* in the presence of 100 μM uric acid + 10 μM vitamin C; *lane j*: as in *lane h* + 100 nM platelet activating factor-16 (PAF-16); *lane k*: as in *lane j* + 100 μM uric acid + 10 μM vitamin C; *lane l*: simultaneously activated platelets and PMNs (same blood cell numbers as in *lanes c* and *d*); *lane m*: standardized supernatant of simultaneously activated platelets and PMN. Data are means ± SD for $n = 7–8$ experiments. $^{**}P < 0.001$; no asterisk indicates $P > 0.05$ (differences between SC-PAO or SC-PVO vs. control in all cases).

While the L_P of SC-PAO did not change significantly under any of the various additional conditions (Fig. 1, *lanes b-e*, *l*, and *m*), that of SC-PVO changed substantially depending on the incubation conditions. As is evident from Fig. 1, *lane b*, thrombin, the key enzyme of coagulation, even at the high concentration of 1 IU/ml, did not increase L_P of pure cultures, which were those normally investigated (see also Supplemental Video S1; Supplemental Material for this article is available online at the *Am J Physiol Heart Circ Physiol* website). The L_P

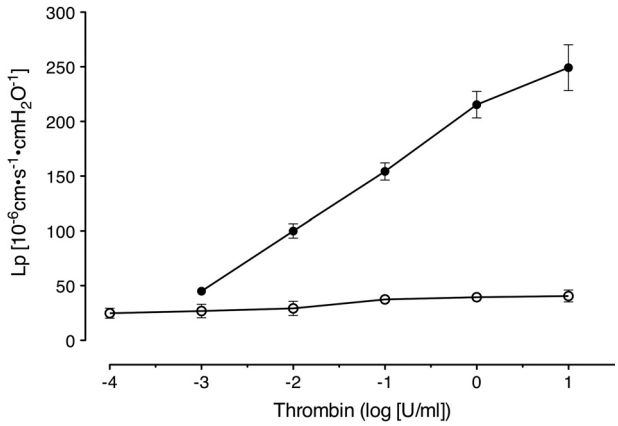

Fig. 2. Influence of thrombin and contaminating pericytes on the hydraulic conductivity (L_P) of SC-PVO. ○, SC-PVO with pure endothelial tissue and a loose pericyte network on the contralateral surface of the filter. ●, Similar experiments on sandwich cultures in which the endothelial cell layers were contaminated by ~3% pericytes. Data are means ± SD; $n = 4$.

increased considerably and concentration dependently, however, in response to thrombin if the endothelial sheets were contaminated by >3% pericytes (Fig. 2). Microscopic inspection revealed occasional thrombin-induced contraction of individual pericytes, resulting in "holes" in the endothelial sheet. No changes in L_P were observed when SC-PVO were exposed to ADP-activated platelets (Fig. 1, *lane c*). FMLP-activated PMN (cell density 10-fold higher than venular endothelial cells), however, induced an approximately twofold increase of L_P (Fig. 1, *lanes d* and *e*) but only when activated in the presence of 10 μM H_2O_2 (which itself, like FMLP, had no effect on L_P). The L_P response of SC-PVO to activated PMN/H_2O_2 was abolished by antioxidants such as uric acid (Fig. 1, *lane f*) or QG (Fig. 1, *lane g*). In contrast, in the presence of 100 nM AA (which itself had no prompt effect on barrier function), the deleterious effect of FMLP/H_2O_2-activated PMN (analogous cell densities as in the experiments before) on L_P was increased twofold (Fig. 1, *lane h*), and, after additional application of PAF, an important mediator of inflammation (104), L_P increased four- to fivefold (Fig. 1, *lane j*) compared with untreated cultures (Fig. 1, *lane a*). Neither of these effects could be prevented by antioxidants (such as uric acid and vitamin C; Fig. 1, *lanes i* and *k*, respectively). The fastest breakdown of the SC-PVO was observed after exposure to simultaneously activated platelets and PMNs (platelet density 30-fold that of the PMN; Fig. 1, *lane l,* see also Supplemental Videos S2–4). Similar changes in SC-PVO L_P were induced by exposure to the standardized supernatant of the simultaneously activated platelets and PMNs (Fig. 1, *lane m*).

Figure 3 shows a series of phase-contrast images from a time-lapse recording (see MATERIALS AND METHODS) of the reactions of a human coronary endothelial cell islet (surrounded by pericytes not visible in the frames) during some of the above, almost identical incubation conditions. Additions were made

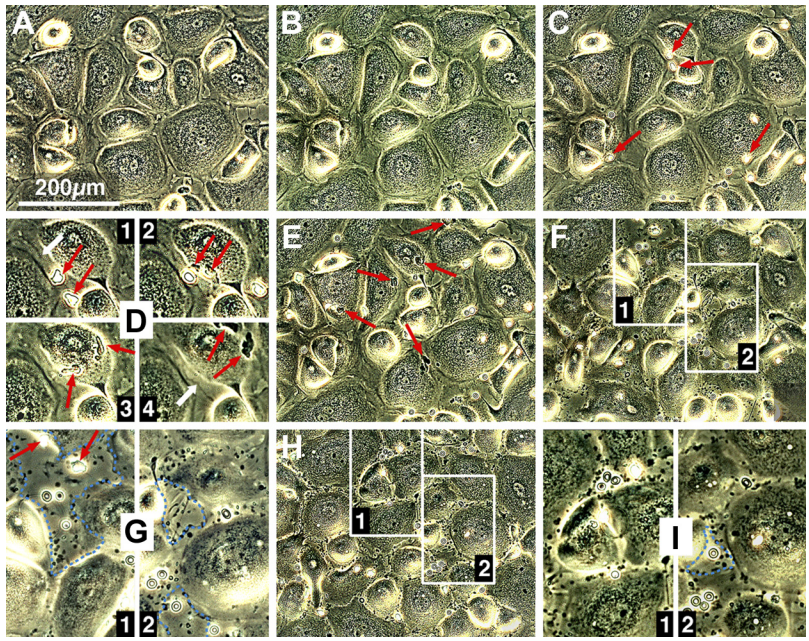

Fig. 3. Reactivity of cultured human endothelium of postcapillary origin. Specific reactions of venular endothelial cell (VEC) to activated blood components and to QG are reflected in the endothelial tissue architecture, which is constantly remodeled under control conditions. Additions were made successively, i.e., the previously added components remained in the chamber. *A*: control. *B*: after 3- min exposure to thrombin (1 IU/ml). *C*: 30 min after addition of unstimulated PMNs (~1/1 VEC), which initially appeared as loosely attached, golden corpuscles predominantly at the apical endothelial surface (some are marked by red arrows). *D*: 2 PMNs (red arrows) transmigrate the endothelial layer via an intercellular junction (white arrow). Four successive exposures were taken at 5-min intervals. *E*: activated PMNs 15 min after addition of FMLP; the leucocytes (red arrows) that had emigrated are following the chemotactic gradient of their activator and are migrating back to the incubation medium (watch Supplemental Video S3). *F*: 15 min after the addition of platelets (small, unattached ellipsoid corpuscles predominantly along the endothelial clefts), many venular endothelial cells are contracted and a widespread disruption of their clefts is evident; the *frames 1* and *2* in *f* are shown enlarged in *G*, individual platelets (black corpuscles) within enormously opened endothelial clefts (encircled by dotted blue lines) adhere to the substratum but do not aggregate. *H*: 60 min after the addition of QG individual endothelial cells are relaxed and flattened again and their junctions are almost completely reclosed. *I*: enlarged *frames 1* and *2* from *h*. Phase-contrast micrographs (*A–I*) are discrete frames from time-lapse video sequences included in Supplemental Videos S1–5.

successively without removing the prior supplements. Endothelial tissue grown under optimized and strictly standardized conditions, i.e., unperturbed, showed the typical paving-stone-like tissue architecture (Fig. 3*A*), which remained similar to control during exposure to thrombin (Fig. 3*B*), nonactivated PMNs (Fig. 3, *C* and *D*), and PMNs activated with FMLP in the absence of H_2O_2 (Fig. 3*E*). Many PMNs transmigrated soon after their contact with endothelial cells into the subendothelial space, and the detailed behavior of two of them is shown in Fig. 3*D*. The addition of the formylated peptide, however, increased the amoeboid motility of the PMNs about fivefold (1.3 ± 0.2 vs. 6.2 ± 0.9 μm/min), and all leucocytes rapidly followed the chemotactic gradient of their activator and migrated quickly back into the incubation medium. The addition of platelets caused the intercellular clefts to open promptly (Fig. 3, *f* and *g*). This breakdown of the endothelial barrier was reversed by the addition of QG (Fig. 3, *h* and *i*) despite the continued presence of thrombin and activated PMNs and platelets. The complete time-lapse recordings are available in Supplemental Videos S1–5.

Figure 4 demonstrates the assembly of F-actin in sheets of human postcapillary venular endothelial cells (again cocultured with surrounding pericytes, not visible) as revealed after being washed, fixed with formaldehyde, permeabilized with Triton X-100, and stained with fluorescent phalloidin (red). In the presence of activated platelets and PMNs (Fig. 4, *C* and *D*), the degree of actin polymerization in venular endothelial cells is increased substantially compared with quiescent cells with their typical thick cortical actin ring (Fig. 4, *A* and *B*). Following incubation with 50 μM QG for 2 h, the F-actin in the endothelial cells was, however, completely disaggregated. Using a longer (eightfold) exposure time in these images to document the weak actin fluorescence of these cells (Fig. 4, *E* and *F*) shows that the activated PMNs (some marked by white arrows in Fig. 4*F*) appear as brightly fluorescent corpuscles despite their low concentration of actin (10% of that of resting endothelial cells under standard conditions) and the actin in the leucocytes remained in the polymerized form. The actin systems in control endothelial cultures also disassembled completely on incubation with QG (50 μM; Fig. 4*G*). With respect to Fig. 4, it must be noted that the unavoidable preparation and fixation of venular endothelial cells for these studies led frequently to a final contraction and hence distinct gap formation between these highly reactive cells. At first glance, this may erroneously create the impression that the starting cell layer was either not tight or nonconfluent or that QG did not tighten the tissue barrier in such experiments.

Pharmacological Studies

To gain deeper insight into the metabolical and cellular origin of the release products of the activated blood cells in SC-PVO, the cocultures were incubated with various specific inhibitors (Fig. 5, *lanes a–l*). These experiments were based on considerations relating to metabolic cooperation between en-

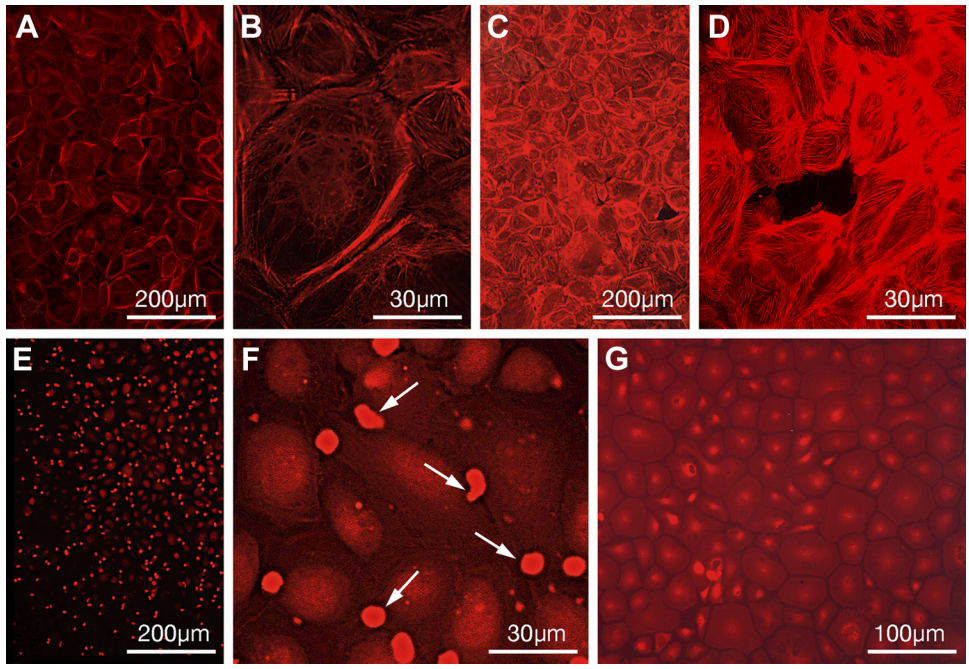

Fig. 4. Assembly of α-actin in postcapillary VEC under various conditions. All preparations were stained with immunofluorescently labeled phalloidin (red). Overview of a quiescent culture under standard in vitro conditions (*A*; 37°C, incubation in filtration medium) and cells of such a culture at higher magnification revealing the typical cortical actin rings (*B*). *C*: overview of a culture after 10-min incubation with simultaneously activated PMNs and platelets. *D*: enlargement showing the rapid polymerization of actin structures and the transition to the activated endothelial phenotype with thin cortical actin and abundant stress fibres. In the center of the image, VEC contraction has led to the localized separation of the first intercellular junctions. This would be apparent in vivo as the breakdown of the venular barrier at this point. *E*: overview of a culture after addition of activated platelets, PMN, and QG (50 μM) after a 2-h incubation. *F*: QG does not restore cortical actin but suppresses F-actin of both cortical structures and stress fibers. A small area of the same culture as in *E* at high magnification. White arrows point to comparatively brightly labeled PMN; platelets appear as much smaller red particles. *G*: control for *E* and *F*, here the endothelial cells were incubated under standard culture conditions (absence of the activated blood cells) but in the presence of 50 μM QG. Both actin systems again disassembled completely.

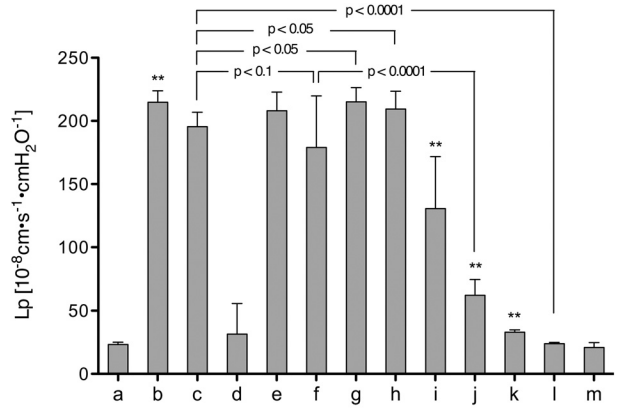

	a	b	c	d	e	f	g	h	i	j	k	l	m
platelets + PMN	-	+		+								+	-
supernatant	-		+		+	+	+	+	+	+	+		-
ASA	-			+	+								-
5-LOX inhibitor	-						+						-
FLAP inhibitor	-							+					-
LTB_4 receptor antagonist	-								+	+			-
PAF-16 antagonist	-					+				+			-
Quercetin glucuronide	-										+	+	+

Fig. 5. Pharmacological interference with intracellular eicosanoid metabolism. All measurements were started promptly after the addition of the inhibitors and continued for 30-min at 37°C. *Lane a*: control (serum-free medium); *lane b*: cultures incubated simultaneously with PMNs and platelets under standard conditions in the presence of FMLP and ADP to activate the blood cells (cf. Fig. 1, lane *l*): *lane c*: cultures incubated with 1:10 diluted supernatant of exogenously activated platelet/PMN; *lane d*: as in *b* but in the presence of 500 μM acetylsalicylic acid (ASA). In all the subsequent experiments, cultures were incubated with the same supernatant as in *lane c*, but with the following additives: *lane e*: 500 μM ASA; *lane f*: 100 μM PAF-16 antagonist; *lane g*: 100 μM ZD2138 [5-lipoxygenase (5-LOX) inhibitor]; *lane h*: 100 μM BAY-X-1007 [5-lipoxygenase-activating protein (FLAP) inhibitor]; *lane i*: 1 μM U-75302 [leukotriene B_4 (LTB_4) receptor antagonist); *lane j*: additives of *lane f* + *lane i* together; *lane k*: 100 μM QG; *lane l*: addition of simultaneously activated platelets + PMNs in the presence of 100 μM QG; *lane m*: as in *lane l*, but in the absence of the supernatant. Data are means ± SD; $n = 7–8$ experiments. $^{**}P < 0.001$; no asterisk indicates $P > 0.05$ (differences vs. control in all cases unless otherwise indicated).

dothelial cells, platelets, PMN, and erythrocytes (see Fig. 11 for summary).

The observed breakdown of the SC-PVO barrier in the presence of simultaneously activated platelets and PMNs or their supernatant (Fig. 5, *lanes b* and *c,* respectively) could be blocked almost completely when platelets were preincubated with ASA (500 μM) before addition to SC-PVO (Fig. 5, *lane d*). In contrast, pretreating the PMNs with ASA and then coculturing them with platelets in SC-PVO had no acute inhibitory influence on L_P (data not shown). While the effect of the L_P-increasing platelet/neutrophil-release products in the supernatant of the blood cells could not be inhibited by addition of ASA (Fig. 5, *lane e*), the addition of PAF antagonist (Fig. 5, *lane f*) or inhibitors of leukotriene synthesis (Fig. 5, *lanes g* and *h*) to SC-PVO in presence of the supernatant from prestimulated platelets and PMNs had also no statistically relevant effects. In contrast, addition of the LTB_4 receptor antagonist U-75302 attenuated the L_P increase significantly (Fig. 5, *lane i*). The tightness (lowering of L_P) of the venular wall models increased further when U-75302 was added together with the PAF antagonist (Fig. 5, *lane j*). On the other hand, 100 μmol/ml QG proved to be a very effective inhibitor of L_P increases, not only in SC-PVO incubated with platelets and PMNs (Fig. 5, *lane k*), but also, in sharp contrast to ASA, in SC-PVO jeopardized by the addition of the supernatant of

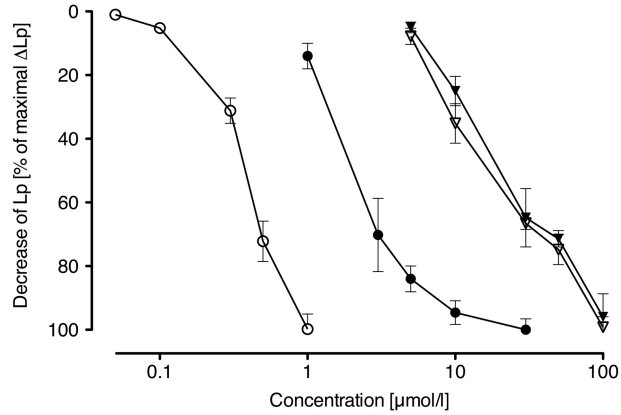

Fig. 6. Concentration-response relations for the repair of leaky postcapillary venular wall barriers in vitro by QG, ASA, and LXA_4. QG (▽), ASA (▲), and LXA_4 (○) reduced platelet/PMNs release product-induced increases in L_P of human SC-PVO. QG and LXA_4 act synergistically (●). In this experiment, the concentration of QG was varied while that of LXA_4 was kept constant (10 nM). Concentration axis refers to QG, LXA_4 was 10 nM in all experiments. Data are means ± SD; $n = 7–9$.

the activated blood cells (Fig. 5, *lane l*). QG itself did not influence basal barrier function (Fig. 5, *lane m*).

Influence of ASA and QG on Platelet/PMN-Induced Increases of L_P of SC-PVO and the Effect of Lipoxin A_4

Figure 6 shows the concentration dependency of the inhibitory effect of ASA and QG on platelet/PMN-supernatant-induced increases of L_P (curves at the *right*) and similar experiments with lipoxin A_4 (LXA_4) which reached maximum inhibitory potency at 1 μM (*left*). Interestingly, the concentration/response curve of QG (but not that of ASA, data not shown) was shifted in the presence of 10 nM LXA_4 to lower concentrations (central curve) by about an order of magnitude (synergism).

Figure 7 shows the time dependency of QG-induced repair processes in SC-PVO that had been completely opened by

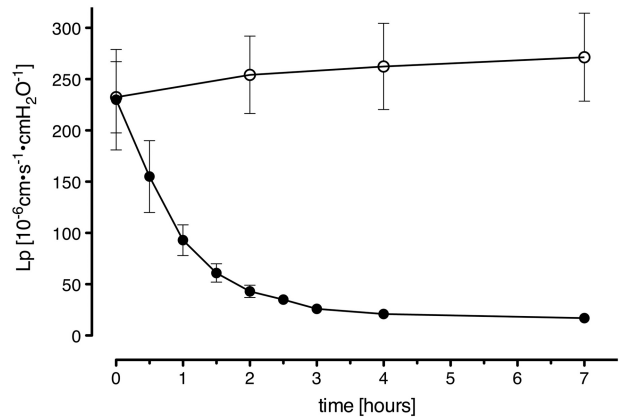

Fig. 7. Barrier function of SC-PVO during extended exposure to supernatant of activated PMNs and platelets in the absence (○) or presence (●) of QG. Sandwich cultures were previously exposed to standardized supernatant to induce maximum contraction and a correspondingly high L_P, and then further incubated in the absence or presence of 50 μM QG. QG induced prompt repair of the endothelial layer after ~6–8 h L_P had declined to values typical of unstimulated postcapillary venular wall barriers in vitro. In contrast control SC-PVO remained leaky throughout the experimental period.

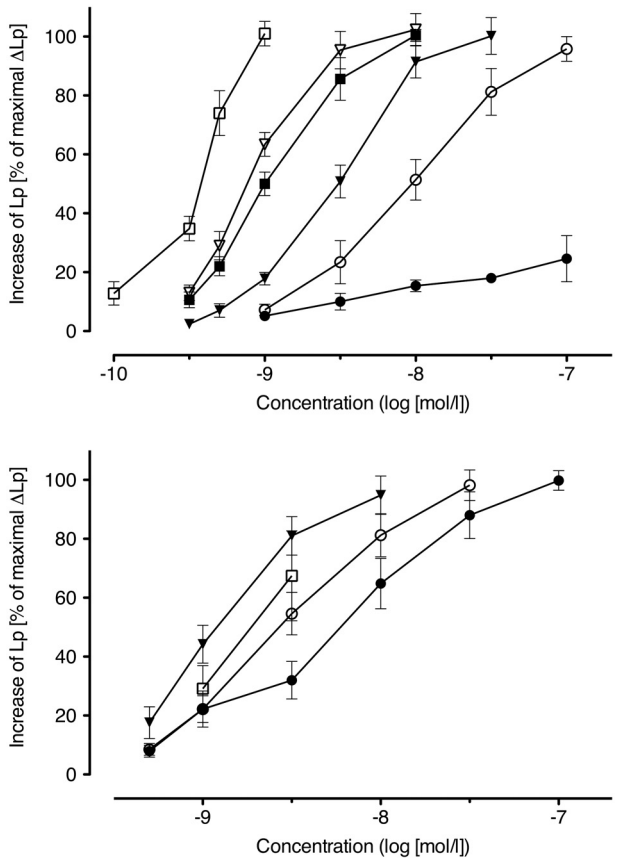

Fig. 8. Inflammatory mediators increase the L_P of SC-PVO concentration dependently and synergistically. Ordinate shows the increase in L_P in the first 20 min of the linear phase of the response above that in medium without supernatant. This difference was referred to the maximum L_P response (achieved with 100 nM LTB_4), the latter defined as 100%. *Top*: L_P response to PGE_2 (○); PAF (●); LTB_4 (▽); LTB_4 + 3 nM PGE_2 (■); LTB_4 + 3 nM PAF (▽); and LTB_4 + 3 nM PAF + 3 nM PGE_2 (□). *Bottom*: L_P response to: IL-8 (●); IL-6 (○); IL-6 + 0.3 nM LTB_4 (▼); and IL-8 + 0.3 nM LTB_4 (□). Data are means ± SD; n = 7–9.

prior incubation with the supernatant of simultaneously activated platelets and PMN. After ~6–8 h, such layers revealed again the typical tightness of resting venular endothelium. In the controls, the endothelial barrier remained open (the initial L_P even increased), and occasionally the venular endothelial cells detached from their substratum.

Influence of Various Mediators of Acute Inflammation on the L_P of SC-PVO

L_P of SC-PVO increased characteristically and concentration dependently on exposure to various lipid and peptide mediators of acute inflammation, some of which cooperated synergistically with respect to opening of these postcapillary venule barriers in vitro (Fig. 8). In combination with LTB_4, minimum concentrations (3 nM) of both PAF and PGE_2 (separately or in combination) shifted the concentration/effect curve for LTB_4 synergistically by almost an order of magnitude to lower concentrations (Fig. 8, *top*). Similarly, IL-6 and IL-8 caused a concentration-dependent loss of barrier function and acted synergistically with LTB_4 (Fig. 8, *bottom*).

Influence of Various Inhibitors on the Release of Eicosanoids During the Metabolic Cooperation between PMNs and SC-PVO in the Presence of AA and PAF

The foregoing experiments with inhibitors suggest that the release products from activated platelets, most probably AA and PAF, stimulate the synthesis and release of a leucotriene from simultaneously present activated PMNs. To gain insight into the eicosanoids actually released in the vessel wall model under such incubation conditions, SC-PVO were first preincubated for 4 h in medium containing the supernatant from activated platelets and PMNs, thus mimicking acute inflammatory conditions. The incubation was then continued in fresh medium (filtration medium) in the presence of PMNs and the typical platelet release products AA (20 μM) and PAF (100 nM). The release of LTB_4, PGI_2 and PGE_2 could be demonstrated; addition of inhibitors of eicosanoid synthesis had the expected characteristic effects (Fig. 9).

Further experiments revealed that red blood cells also played an important role in these transcellular metabolic interactions (results not shown in Fig. 9). In the presence of these cells (1,000-fold greater density than the PMNs in the mixed cultures), trace amounts of cysteinyl leucotrienes (<30 pg/ml) such as LTC_4 were no longer detectable in the incubation medium of activated SC-PVO and PMN, but the concentration of LTB_4 measured in the presence of erythrocytes was roughly fourfold that in the absence of these cells (compare with Fig. 9*B*).

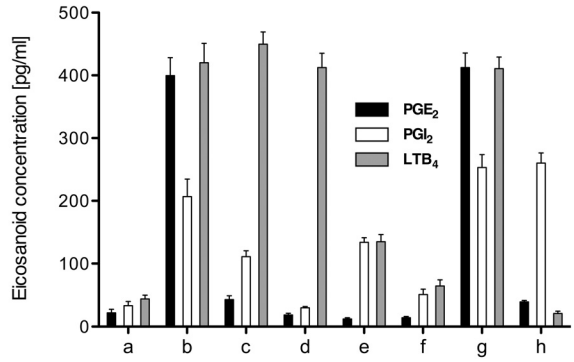

PMN + AA + PAF-16	-	+	+	+	+	+	+	+
ASA	-		+					
Rofecoxib	-			+				
Quercetin glucuronide	-				+			
5-LOX inhibitor	-					+		
LTB_4 receptor antagonist	-						+	
FLAP inhibitor	-							+

Fig. 9. Eicosanoids released during the metabolic cooperation between PMNs and SC-PVO. Extracellular accumulation of PGE_2, PGI_2, and LTB_4 (black, open, and gray columns, respectively) in the apically applied incubation medium was investigated in resting SC-PVO (*lane a*) and in activated SC-PVO (*lane b*; preincubation for 4 h with platelet/neutrophil-supernatant and subsequent washing) in presence of PMNs and AA (20 μM) and PAF-16 (100 nM). Pattern of the release products during analogous preincubation and subsequent exposure to PMN/AA/PAF could be altered characteristically in presence of ASA (*lane c*), rofecoxib (*lane d*), QG (*lane e*), each 100 μM; or ZD2138 (*lane f*), U-75302 (*lane g*), and BAY-X-1007 (*lane h*), each 10 μM for 1 h. Eicosanoid concentrations were measured using ELISA. Data are means ± SD; n = 7–9.

Segregation of Activated Platelets and PMNs and the Protective Effect of QG in the Inflamed Microvasculature of Isolated Blood-Perfused Human Hearts

Enzyme histochemical discrimination of arterioles and venules and immunologic staining of PMNs and platelets in three human hearts revealed selective segregation of PMNs in the venules and their surrounding interstitium (Fig. 10, *A* and *B*) and of platelets in the corresponding arterioles (Fig. 10, *A* and *B*) after circumfusion of the ventricular coronary system with matched whole blood for 10 min. To activate the two blood cell species maximally and simultaneously, 100 μM ADP and 1 μM FMLP were added to the blood. Similar results were obtained in two further hearts in which only exogenous ADP was added to activate the platelets selectively (micrographs not shown). The release products of these cells also promptly activated the PMN. In contrast, accumulation of platelets as well as PMNs was practically absent when 100 μM QG was added to the recirculated blood (followed after 5 min) by addition of 100 μM ADP and 1 μM FMLP (3 hearts, Fig. 10*E*). However, FMLP-activated PMNs could still be recruited from coronary venules into the myocardial interstitium of reperfused human heart tips (Fig. 10*F*).

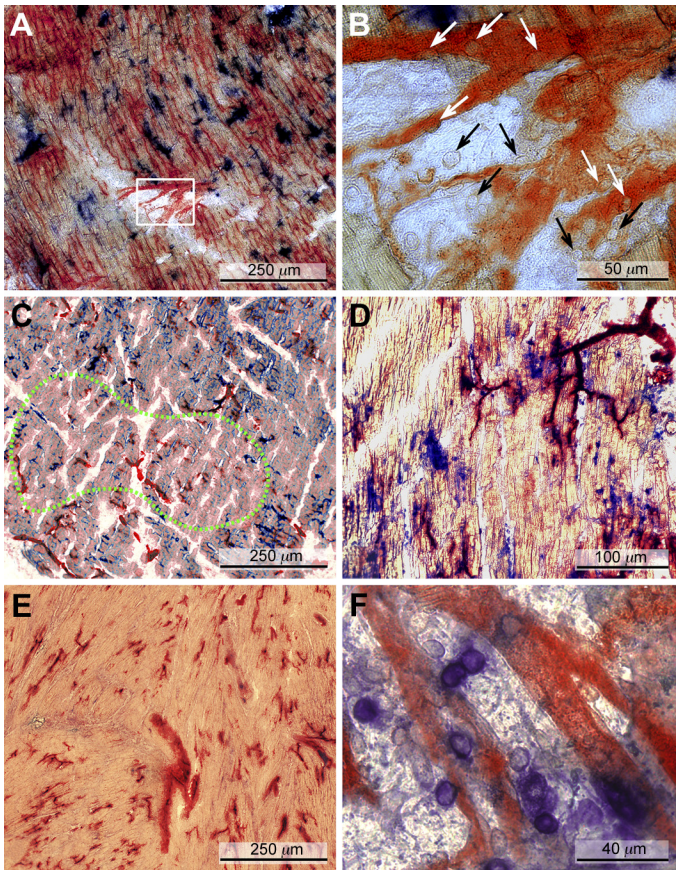

Fig. 10. Microvessel-specific segregation of simultaneously activated platelets and PMNs in the blood-perfused human heart. Bright-field microscopic images with the exception of the phase-contrast view in *B*. All preparations were circumfused for 10 min with matched whole blood in the presence of 100 μM ADP and 1 μM FMLP (to activate the platelets and PMN, respectively) and in the absence or simultaneous presence of QG (50 μM). *A* and *B*: immunohistochemical stains showing platelet aggregates (dark blue) in the otherwise unstained arterioles. Postcapillary venules could be visualized enzyme histochemically by their rust-red staining for DAP. *A*: overview. *B*: higher power view of the frame in *A*: no platelets are present in postcapillary venules. This phase-contrast image shows adherent PMNs ready for diapedesis inside these vessels (some marked by white arrows) and in addition many emigrated leukocytes accumulating in the interstium (black arrows). *C* and *D*: immunohistochemical staining for platelet aggregates (blue) selectively within the smallest arterioles (brick-red staining for AP) and the respective postarteriolar capillaries. *C*: overview, the unstained postcapillary venules contain no platelet aggregates and hence appear relatively "empty" (area within the dotted green line). *D*: region in the vicinity of an arteriole at high magnification. Individual PMNs are now visible (violet). Many emigrating PMNs accumulate around the otherwise unstained venules, the brick-red arterioles in their vicinity are free of these leucocytes. *E* and *F*: similar histochemical studies in the presence of QG (stains analogous to *C* and *D*). *E*: aggregates of platelets cannot be detected in the arterioles. *F*: emigrated PMNs (violet) after activation with FMLP.

DISCUSSION

In the present study, sandwich cultures of the constituent cells of human myocardial arteriolar and venular vessel walls and a custom-made filtration system (63) allowed acute inflammatory processes to be modeled in vitro. Pharmacological and biochemical studies were employed to elucidate the participating mechanisms and to characterize potential means for therapeutic intervention.

Studies on the Hydrodynamic Resistance of Cultured Microvascular Tissue Barriers

The baseline L_P of sandwich cultures of endothelial cells and pericytes of postcapillary venular origin (SC-PVO), $2.55 \pm 0.32 \cdot 10^{-7} cm \cdot s^{-1} \cdot cmH_2O^{-1}$ ($n = 10$), was consistent with the L_P of intact venules in vivo (39, 67, 73). The basal L_P of analogous tissue barriers of precapillary arteriolar origin (SC-PAO), $3.24 \pm 0.52 \cdot 10^{-8} cm \cdot s^{-1} \cdot cmH_2O^{-1}$ ($n = 37$), was about an order of magnitude lower, presumably reflecting both the higher degree of organization of the intercellular junctions of the arteriolar endothelium (84, 85) and the presence of a thick and continuous ECM organized by the subendothelial arteriolar pericytes (63). The characteristically low L_P of the precapillary arteriolar vascular barrier in vitro did not change significantly under any of the subsequent experimental conditions and remained consistent with that reported for the tight arterioles of the rat brain and mesentery (39, 40).

As is typical for isolated venules from human myocardium, SC-PVO possessed a wide-meshed pericyte network with an only weakly developed ECM. The barrier properties in this model (63) thus presumably reflected primarily the properties of the contractile endothelium. In contrast to the SC-PAO, the L_P of the venular model, relatively low under basal, quasi-physiological conditions, proved to be highly dependent on the composition of the incubation medium.

Influence of thrombin. Even high concentrations of thrombin (1 U/ml; full activity in culture medium containing the plasma derivative Biseko instead of FCS) had no permeability-enhancing effect on SC-PVO. This finding is consistent with the observation that acute exposure to a very high thrombin concentration (10 U/ml) does not increase venular permeability in situ but only after 24-h adaptation of the microvasculature to locally developing inflammatory reactions (17). A plausible explanation for this observation may be deduced from our findings relating to the influence of inflammatory cells and mediators on the wall tightness of the venular wall model (see below). *1*) The observed lack of influence of thrombin on the barrier function of SC-PVO is in clear contrast to many studies

(27, 59) in which thrombin has been used successfully to enhance endothelial permeability in vitro. One explanation for this discrepancy might be that the endothelial barriers studied during those investigations contained admixtures of contaminating cells that contract on contact with thrombin. As seen in Fig. 2, the presence of very few pericytes (3% of the total cell number) is sufficient to elicit large changes in permeability of the entire endothelial sheet. *2*) Other reasons for the observed discrepancy can be deduced from the fact that we employed new culture techniques. Sandwich cultures of human arteriolar and venular endothelial cells with their corresponding pericytes (63) provide local growth conditions for the isolated endothelial cells which mimic the situation in vivo more closely. *3*) Yet a further contribution to the discrepancy between our observations and the literature cited is that endothelial cultures grown in serum-containing media already show signs of inflammatory activation, such as elevated expression of dipeptidyl aminipeptidase IV, leucocyte adhesion molecules such as ICAM-1, polymerized smooth muscle α-actin, and an increased L_P (63). Serum in fact contains many inflammatory mediators (release products of activated platelets and leucocytes, activated coagulation factors, etc.). In the present study, we therefore cocultured exclusively homogenous sheets of endothelium and pericyte-networks and preincubated these "sandwich-filters" in a serum-free medium that contained a human plasma derivative without coagulation factors or isoagglutinines for 2 days before the experiments.

Influence of platelets. Platelets have been regarded in the literature as promoters of high vascular tightness (88), and the tightness of our sandwich cultures in presence of platelets was indeed similar to control (see Fig. 1, *lane c*). In contrast, in the mouse, a key role for activated platelets as inducers of a higher permeability of lung endothelium and a concomitant leakage of plasma proteins has been reported (89, 102). The behavior of platelets, however, depends critically on the balance between platelet-activating and platelet-inhibiting substances in their immediate vicinity. In the present experiments, they were activated with ADP, which is rapidly metabolized by venular endothelial ecto-phosphatases to adenosine, a potent platelet inhibitor (29, 62, 65). Adenosine accumulation at the endothelial surface might therefore have been causally involved in the protection of the postcapillary endothelium.

Our histological studies in isolated perfused, human heart tips show platelet aggregation only in the arterioles. The released ADP, together with the exogenous ADP, is presumably again degraded to adenosine during the passage through the capillary bed, resulting in a high adenosine concentration in the venules. The selective accumulation of ADP-induced platelet aggregates in the arterioles might be explained by the expression of specific, shear force-dependent platelet receptors on the arteriolar endothelium (3, 94). Moreover, cultured human endothelial cells of arteriolar origin contain, in contrast to those of venular origin, particularly high numbers of Weibel-Palade bodies (63). The content of these secretory organelles (56) is dominated by the hemostatic factor von Willebrand factor antigen (vWF:Ag), which strongly promotes platelet adhesion to the vessel wall (20).

Influence of PMNs. PMNs have been regarded frequently as being responsible for oxidative vascular damage, which leads to increased permeability (33, 36, 89), particularly after ischemia/reperfusion (69, 71, 103). However, we were able to demonstrate such an effect only when the leucocytes had been incubated together with exogenous H_2O_2 (which itself had no influence), thereby enhancing their potency for the formation of reactive oxygen species (ROS). A similar dependency has been reported for PMN, which are thought to cause postischemic dysfunction of isolated perfused hearts via formation of hypochlorous acid in the simultaneous presence of thrombin and H_2O_2 (69).

In our hands, however, accumulation of ROS could be prevented completely by uric acid, vitamin C, or quercetin glucuronide. Uric acid is a typical release product of endothelial cells (61, 62), its physiological plasma concentration (~100 μM) is very high, and it is a very powerful antioxidant (8). The pathogenetic significance currently attributed to ROS and nitric oxidde (NO) metabolites may thus be overestimated.

Influence of simultaneously activated platelets and PMNs. The permeability-enhancing effect of highly purified PMNs was potentiated in the presence of H_2O_2 and exogenous AA (typically released by activated platelets), and the increase in L_P could not be prevented by antioxidants. This effect of AA was promoted by addition of PAF.

The most dramatic increases in SC-PVO L_P, however, occurred during their interaction with concurrently activated platelets and PMNs (Supplemental Video S4). Coupling between leucocyte/platelet activation and microvessel permeability, thrombosis, and inflammation in vivo is attracting increasing interest and is subject of several excellent reviews (33, 47, 90). Studies (51, 52) using silver staining have demonstrated directly selective and uniform opening of postcapillary venular endothelial junctions under the influence of inflammatory mediators. These substances might well be mainly release products from activated platelets and PMN, such as PAF and LTB_4 (see below). As noted above, this could then explain why the postcapillary venular barrier breaks down (17, 51) when these acutely activatable blood cells accumulate in inflamed microcirculatory regions and are then exposed to thrombin, the most potent natural platelet activator.

Contractility of Venular Endothelial Cells, Loss of Their Barrier Function, and Specific Pharmacological Intervention

The observed wide and general opening of junctions during contraction of venular endothelial cells with involvement of polymerized α-actin is consistent with other studies (13, 26, 43, 91, 95). The quiescent endothelial phenotype is characterized by a thick cortical actin ring. Stress fibers are practically absent. In contrast, the activated cell phenotype expresses abundant stress fibers and only little or even no cortical actin. A whole plethora of inflammatory events triggers this reorganization, whereby the phosphorylation of the myosin light chain (MLC) is considered to be centrally important and directly correlated with the state of contractility. The latter depends not only on the activity of a specific myosin light chain kinase (MLCK; Ref. 82), but also of the activity of the corresponding phosphatase (MLCP). This enzyme activity is tightly coupled to activated RhoA, which enhances the phosphorylation of the phosphatase regulatory subunit via a special Rho kinase (9). This kinase itself can also phosphorylate MLC (2). The current paradigm holds that the tightness of an endothelial barrier is maintained by the finely tuned equilibrium between the forces providing centripetal tension (actomyosin

contraction depending on stress fibers) and the centrifugal forces, which rely on several cytoskeletal components coupled to the cortical actin ring. The latter is necessary for the establishment of intercellular adhesion and the maintenance of endothelial barriers (13). Some of them are represented by adhesion molecules, which provide cell-cell and cell-substrate attachments. Of particular interest in this context is our observation that both activated and quiescent venular endothelial tissue lose their typical actin systems during incubation with QG and simultaneously develop surprising tightness (i.e., low L_P, compare Fig. 5, *lanes k–m*). Interestingly, another study (1) has raised the possibility that, in addition to the assembly and complex regulation of the actin/myosin system, certain factors may contribute to the opening of endothelial clefts of isolated venules in response to inflammatory mediators such as PAF and bradykinin. In that study, it was suggested that there are extensive subpopulations of endothelial cells that regulate the width of the intercellular clefts by varying the conformation of specific adhesion molecules. The mode of action of QG will, however, remain unclear until the signal transduction cascade has been fully elucidated.

The contractility of the venular endothelium has long been recognized (26, 31, 41), and although studies (31, 92) have emphasized repeatedly that this endothelial activity represents an important pharmacological target, this concept has not yet found wide acceptance. Thus, while in the context of the development of new antithrombotic medications great emphasis is currently being placed on development and clinical introduction of specific thrombin inhibitors (54, 55), very little attention is being paid to sealing of the venular endothelium and hence shielding the coagulatory zymogens in plasma from the subendothelial pericytes with their highly concentrated tissue factor that plays the key role in triggering of intravasal coagulatory processes (14, 38, 48, 64).

Identification of LTB_4 as a Mediator Deleterious to the Venular Barrier

Effect of ASA and inhibitors of leucotriene synthesis on the release of permeability-enhancing products from simultaneously activated platelets and PMN. The initial studies using ASA indicated that at least one major substance component, probably AA, was released selectively from activated platelets, which PMNs then used for the synthesis and release of at least one permeability-enhancing, stable derivative. The studies with the 5-LOX inhibitor ZD2138 or the FLAP inhibitor BAY-X-1007 indicated that the liberated compound was probably a leucotriene.

Effect of PAF and LTB_4 receptor antagonists. Application of the highly specific PAF antagonist 1-*O*-hexadecyl-2-acetyl-*sn*-glycero-3-phospho-(*N*,*N*,*N*,-trimethyl)hexanolamine (23) to the filtration medium indicated that PAF itself did not induce a prompt or statistically relevant enhancement of permeability of cultured human venular endothelial cells (Fig. 5, *lane f* and Fig. 8, *top*). This finding agrees well with those of Curry et al. (17) but is in contrast to other findings on the biological effects of PAF (1, 95, 104). It is well accepted, however, that PAF of platelet origin can increase production and release of LTA_4 in PMNs (44, 93), which is a precursor of LTB_4 synthesis in endothelial cells (75), erythrocytes (53), and, to a minor extent, in the PMNs themselves (76). This is consistent with the present results showing a greater influence of PMNs on the L_P of SC-PVO during incubation with AA and PAF (see Fig. 1, *lane j*). In addition, it also appears reasonable that the concurrent presence of the LTB_4 receptor antagonist U-75302 and the above-mentioned PAF antagonist almost completely prevented the breakdown of the barrier function of SC-PVO in the presence of activated platelets and PMNs or their supernatant.

Eicosanoid production and release in SC-PVO cocultured with blood cells. Biochemical analyses strongly imply that LTB_4 is, in fact, a major release product of PMNs in coculture with SC-PVO, when the incubation medium is supplemented with AA and PAF (thus imitating the presence of activated platelets). The fact that considerably larger amounts of LTB_4 were produced under these conditions in the presence of red blood cells is in agreement with earlier studies (53) demonstrating LTB_4 synthesis by erythrocytes incubated with exogenous LXA_4. Interestingly, these findings are also consistent with recent studies in the perfused mesenteric circulation in which hypoxia-induced inflammatory reactions were attributed to the simultaneous action of LTB_4 und PAF (16).

In addition to LTB_4, the prostanoids PGI_2 and PGE_2 are released in large amounts from activated SC-PVO. These products of the COS1 or 2, respectively, have long been recognized as typical endothelial products and strong platelet inhibitors (12). PGE_2 has been reported to potentiate the effects of PAF (30) and to reduce endothelial barrier function (5), observations which could be confirmed by our own results (Fig. 8, *top*).

Synergism Between Various Mediators of Venular Barrier Loss

Barriers formed by SC-PVO and exposed to various inflammatory mediators (PAF, PGE_2, IL-6, and IL-8) separately or in combination showed characteristic concentration-dependent increases in L_P, although the effects were significant only at concentrations far beyond their normal plasma concentrations. In combination with LTB_4, however, a synergistic increase in action of this leucotriene was observed, which, in all probability, also explains the enormous in situ effect of subnanomolar concentrations of LTB_4 on perfused prepared microcirculation systems (77). This effect of the IL-6 and IL-8 is especially interesting. Both peptides are now considered as particularly important participants of acute inflammatory tissue processes in which PMNs are involved (70, 86).

Inhibitory Actions of Quercetin Glucuronide in the In Vitro Model of Acute Inflammation

High concentrations of flavonoids are found frequently as nonessential and healthy plant metabolites in foodstuffs and have attracted interest as natural inhibitors of inflammation (28, 50, 78). A frequently occurring flavonoid is quercetin, which is readily absorbed in the duodenum and then coupled to uronic acid before its transport in plasma (98).

QG is an effective inhibitor of platelet activation via the modulation of PAF synthesis and of glycoprotein VI signaling pathway proteins (6, 99). Moreover, flavonoids like QG have been characterized as efficient inhibitors of 5-LOX (83). In our studies, 100 μM QG inhibited release of LTB_4 and PGE_2, the former possibly reflecting the inhibitory effect of flavonoids on 5-LOX and the latter by the inhibitory effect on platelets. A

direct inhibitory effect of flavonoids on COX-2 has not yet been described and remains speculative.

A strong antioxidant effect has also been ascribed to flavonoid compounds (83), and these compounds have been shown to enhance endothelial NO synthesis (58). QG proved to be an effective antioxidant also in our studies. The inhibitory action of this QG with respect to the recruitment of actin and stress fibers of human postcapillary venular endothelial cells has already been discussed above.

The synergistic increase in endothelium-protective potency of QG by LXA_4, described here for the first time, suggests that QG can act as an efficient inhibitor of platelet/neutrophil-induced edema formation already at relatively low plasma concentrations. LXA_4 at low, basal plasma concentration obviously plays a physiological role as a potent inhibitor of PMNs and in the context of resolution of inflammatory reactions in whole blood (22, 49, 80, 87).

Segment-Specific Microvascular Segregation of Activated Platelets and PMNs During Perfusion of Human Hearts with Whole Blood

As noted earlier, a surprisingly selective segregation of the platelets in arterioles and of the PMNs in postcapillary venules was observed (Fig. 10). In contrast, postcapillary venular endothelium under inflammatory conditions produces plasmalemmal and junctional leucocyte adhesion molecules enabling selective adhesion to and emigration of PMNs from venules (42, 46, 71, 101). Indeed, such leucocytes accumulated abundantly in postcapillary venules and in the local myocardial interstitium around these smallest veins of the hearts investigated, while no wall-resident platelets were apparent. This probably reflects the selective capture of platelets in the corresponding upstream arterioles. The elevated formation and release of PGI_2 and PGE_2 by activated venular endothelium demonstrated in our study (Fig. 9*B*), as well as the formation of adenosine from ADP via endothelial ecto-phosphatases may also, however, have contributed to the prevention of platelet segregation in the lumen of the myocardial venules in the isolated, blood-perfused hearts. The inhibition of platelet aggregation in the vicinity of postcapillary venular endothelium is also in good agreement with time-lapse microcinematographic studies on the respective cellular interactions under defined in vitro conditions (Fig. 3 and Supplemental Videos). Our observations with respect to selective arteriolar segregation of platelets are in contrast to interesting studies showing venular accumulation of platelets after ischemia/reperfusion in blood-perfused microvascular systems in situ (34, 71). While ~25% of the platelets were bound directly to the endothelium, most of the remainder (75%) were bound to PMNs, which might strongly enhance both the metabolic cooperation between these cells and the generation of ROS (71). This cellular interaction probably began already during the ischemia. In our model, however, the platelets encountered the preactivated human arteriolar endothelium abruptly, which obviously reacted by recruitment of vWF:Ag from its particularly numerous Weibel-Palade bodies (see above).

The fact that very similar histological results were obtained when only the platelets were initially activated with exogenous ADP showed that their activation and accumulation in the arterioles of blood-perfused, ischemic hearts will lead spontaneously to the coactivation of PMNs and the venular endothelium. This is very probably initiated by PAF released from the platelets (as shown in Fig. 11).

The fact that (regardless of the activation protocol for the PMNs via FMLP) 50 μM QG completely prevented platelet adhesion and aggregation in the arterioles is consistent with the array of inhibitory actions of this flavonoid discussed above. In addition, these findings could also indicate that the recruitment of p-selectin from Weibel-Palade bodies is specifically inhibited in the arteriolar endothelium by the flavonoid. While the chain of metabolic events leading to the release of PAF and AA from platelets and the coactivation of PMNs and red blood cells to produce LTB_4 should have also been prevented in these hearts (see Fig. 11), the PMNs could still be effectively activated by FMLP. The fact that they then selectively adhered to postcapillary endothelium and emigrated into the myocardial tissue indicates that QG does not on principle impair the important recruitment of these cells for immunological defense purposes.

Synopsis and Physiological Relevance of the Investigated Biochemical Interactions

The newly gained insights into the cellular and molecular interactions of endothelial cells, platelets, PMN, and erythrocytes are outlined in Fig. 11. This scheme also shows the approaches employed in the experiments with inhibitors to elucidate the reactions.

In the vascular outflow from inflamed tissue areas (not shown in Fig. 11), the presence of PAF and LTB_4 will be counteracted in the venous blood by endothelium-derived au-

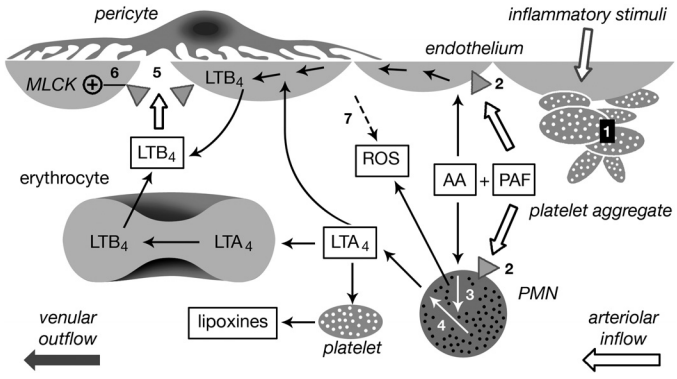

Fig. 11. Scheme of the biochemical and cellular mechanisms proposed to be responsible for the breakdown of the venular endothelial barrier and possible pharmacological intervention. Locally released inflammatory mediators activate the arteriolar endothelium, resulting in the adhesion/aggregation of platelets. PAF released from these platelets activates the arteriolar endothelium further as well as incoming PMN. The latter synthesize leucotriene LTA_4 from AA (also released by the platelets). LTA_4 is metabolized by erythrocytes and endothelial cells to LTB_4, which in turn activates, via specific receptors, the postcapillary venular endothelium. Via complex signal cascades this results, among other enzyme systems, in activation of the myosin light chain kinase (MLCK), contraction of the VEC and widening of the intercellular junctions and hence breakdown of the blood-myocardium barrier. Plasma now flowing into the subendothelial space encounters the pericytes (for the consequences of this, see text). Approaches for pharmacological intervention include *1*: platelet inhibition by ASA; *2*: blockade of the PAF receptor by an antagonist; *3*: inhibition of FLAP; *4*: inhibition of 5-lipoxygenase; *5*: antagonism LTB_4 binding to its endothelial receptor; *6*: intervention (complex) in the actin polymerization process; and *7*: antioxidants against reactive oxygen species (ROS) released by activated PMN.

tacoids such as adenosine, NO, PGI_2, and PGE_2 that are secreted at higher concentrations under these circumstances. These platelet inhibitors also act as potent vasodilators and are therefore very probably mainly responsible for the hyperemic response in the circumference of inflammatory foci. Further downstream in the collecting veins all these compounds are diluted rapidly and are increasingly eliminated by catabolic blood-borne enzymes (PAF, LTB_4, adenosine, and PGE_2) or due to their high innate chemical reactivity (NO) or thermal instability (PGI_2). Correspondingly, the macroscopically evident redness of the hyperemic ring around a typical inflammatory focus, and with it the increased perfusion of the microcirculatory system of this area, diminishes increasingly towards the periphery.

To prevent the penetration of activated defense cells and plasma factors into the remaining circulatory system, it seems also appropriate for the body to isolate an excessive inflammatory focus in the area of its venular outflow. Hence, the release of LTB_4 and PAF and the resulting opening of the venular endothelial barrier not only serve to recruit immunological defense systems but also to activate the coagulation cascade via tissue factor (48, 68) that is expressed particularly on pericytes (14, 38, 64, 97) and that come in direct contact with the zymogens of coagulation in the inflammatory plasma exudate.

Perspectives

The substantial differences in barrier behavior seen in the arteriolar and venular vessel wall models in the present study in response to components of the coagulation or nonspecific immune systems, extrapolated to the intact coronary microcirculation in vivo, strongly imply a key role for the postcapillary venules in myocardial injury or inflammatory processes. Despite their thin walls and loosely organized endothelial cell junctions (18, 84, 85, 96), healthy coronary venules are remarkably tight. This can, however, change drastically on activation, and these specialized vessels can become the hot spots of inflammatory edema, defense processes, and fibrin thrombi. Interventional strategies to prevent the spread of these processes, initially local and aimed at limiting inflammatory reactions and injuries, should primarily address the repair of the damaged blood-myocardium barrier, in particular the venular tightness. In this respect, the mechanism of action of QG and structure/function-relationships needs further elucidation. Promising studies in this direction are the systematic study of quercetin and its derivatives as inhibitors of platelets (99), and the effectiveness of certain polyphenoles, like the flavonoids, as therapeutic agents in systemic sepsis (81). In this illness, activated platelets, PMNs, and the breakdown of the venular barrier in many organs are of key pathogenic importance.

In studies on other blood-organ barriers, including the well-known blood-brain barrier, focusing on the functionally versatile and complexly controlled venular barrier rather than on purely structural aspects might yield new insights.

ACKNOWLEDGMENTS

Marold Buchner and Franz Singer, precision mechanics of the Dept. of Physiology, helped a lot during the preparation and adaptation of special laboratory equipment. The excellent photographic and artwork of Barbara Nees is also gratefully acknowledged.

GRANTS

This work was supported by the University of Munich, by the German Phlebological Society (http://www.phlebology.de), and by a grant of the Friedrich-Baur-Stiftung Munich (info@baur-stiftung.de). The funders had no role in study design, data collection, and analysis, decision to publish, or preparation of the manuscript.

DISCLOSURES

All authors have no possible conflicts of interest with the publication of this article with the exception of S. Nees who has an application for a patent on venular preservation by quercetin glucuronide.

AUTHOR CONTRIBUTIONS

Author contributions: G.J. and S.N. conception and design of research; G.J., D.R.W., M.K., A.S., S.F., E.K., S.L., and S.N. performed experiments; G.J., D.R.W., S.L., and S.N. analyzed data; G.J., D.R.W., T.F., E.K., B.R., S.L., and S.N. interpreted results of experiments; G.J. and S.N. prepared figures; G.J. and S.N. drafted manuscript; G.J. and S.N. edited and revised manuscript; G.J., D.R.W., M.K., A.S., S.F., T.F., E.K., B.R., S.L., and S.N. approved final version of manuscript.

REFERENCES

1. **Adamson RH, Zeng M, Adamson GN, Lenz JF, Curry FE.** PAF- and bradykinin-induced hyperpermeability of rat venules is independent of actin-myosin contraction. *Am J Physiol Heart Circ Physiol* 285: H406–H417, 2003.
2. **Amano M, Ito M, Kimura K, Fukata Y, Chihara K, Nakano T, Matsuura Y, Kaibuchi K.** Phosphorylation and activation of myosin by Rho-associated kinase (Rho-kinase). *J Biol Chem* 271: 20246–20249, 1996.
3. **Andrews RK, Berndt MC.** Platelet adhesion: a game of catch and release. *J Clin Invest* 118: 3009–3011, 2008.
4. **Baetscher M, Brune K.** An in vitro system for measuring endothelial permeability under hydrostatic pressure. *Exp Cell Res* 148: 541–547, 1983.
5. **Baldwin AL, Thurston G.** Mechanics of endothelial cell architecture and vascular permeability. *Crit Rev Biomed Eng* 29: 247–278, 2001.
6. **Balestrieri ML, Castaldo D, Balestrieri C, Quagliuolo L, Giovane A, Servillo L.** Modulation by flavonoids of PAF and related phospholipids in endothelial cells during oxidative stress. *J Lipid Res* 44: 380–387, 2003.
7. **Batra S, Rakusan K, Kuo C.** Spatial distribution of coronary capillaires: A-V segment staggering. In: *Oxygen Transport to Tissue*, edited by Rakusan K, Biro GP, Goldstick TK, Turek Z. New York/London: Plenum, 1989, p. 241–247.
8. **Becker BF.** Towards the physiological function of uric acid. *Free Radic Biol Med* 14: 615–631, 1993.
9. **Beckers CM, van Hinsbergh VW, van Nieuw Amerongen GP.** Driving Rho GTPase activity in endothelial cells regulates barrier integrity. *Thromb Haemost* 103: 40–55, 2010.
10. **Bennett AS, Luft J, Hampton JC.** Morphological classification of vertebrate blood capillaries. *Am J Physiol* 196: 381–390, 1959.
11. **Beutler E, West C, Blume KG.** The removal of leukocytes and platelets from whole blood. *J Lab Clin Med* 88: 328–333, 1976.
12. **Bogatcheva NV, Sergeeva MG, Dudek SM, Verin AD.** Arachidonic acid cascade in endothelial pathobiology. *Microvasc Res* 69: 107–127, 2005.
13. **Bogatcheva NV, Verin AD.** The role of cytoskeleton in the regulation of vascular endothelial barrier function. *Microvasc Res* 76: 202–207, 2008.
14. **Bouchard BA, Shatos MA, Tracy PB.** Human brain pericytes differentially regulate expression of procoagulant enzyme complexes comprising the extrinsic pathway of blood coagulation. *Arterioscler Thromb Vasc Biol* 17: 1–9, 1997.
15. **Cardoso FL, Brites D, Brito MA.** Looking at the blood-brain barrier: molecular anatomy and possible investigation approaches. *Brain Res Rev* 64: 328–363, 2010.
16. **Casillan AJ, Gonzalez NC, Johnson JS, Steiner DR, Wood JG.** Mesenteric microvascular inflammatory responses to systemic hypoxia are mediated by PAF and LTB4. *J Appl Physiol* 94: 2313–2322, 2003.
17. **Curry FE, Zeng M, Adamson RH.** Thrombin increases permeability only in venules exposed to inflammatory conditions. *Am J Physiol Heart Circ Physiol* 285: H2446–H2453, 2003.

18. **Dejana E, Corada M, Lampugnani MG.** Endothelial cell-to-cell junctions. *FASEB J* 9: 910–918, 1995.
19. **Dejana E, Orsenigo F, Molendini C, Baluk P, McDonald DM.** Organization and signaling of endothelial cell-to-cell junctions in various regions of the blood and lymphatic vascular trees. *Cell Tissue Res* 335: 17–25, 2009.
20. **Denis CV.** Molecular and cellular biology of von Willebrand factor. *Int J Hematol* 75: 3–8, 2002.
21. **Faioni EM, Mannucci PM.** Venocclusive disease of the liver after bone marrow transplantation: the role of hemostasis. *Leuk Lymphoma* 25: 233–245, 1997.
22. **Folco G, Murphy RC.** Eicosanoid transcellular biosynthesis: from cell-cell interactions to in vivo tissue responses. *Pharmacol Rev* 58: 375–388, 2006.
23. **Fujii E, Irie K, Uchida Y, Ohba K, Muraki T.** Role of eicosanoids but not nitric oxide in the platelet-activating factor-induced increase in vascular permeability in mouse skin. *Eur J Pharmacol* 273: 267–272, 1995.
24. **Furchgott RF, Zawadzki JV.** The obligatory role of endothelial cells in the relaxation of arterial smooth muscle by acetylcholine. *Nature* 288: 373–376, 1980.
25. **Ganda S.** Microvascular thrombosis and multiple organ dysfunction syndrome. *Crit Care Med* 38: 835–842, 2010.
26. **Garcia JG.** Concepts in microvascular endothelial barrier regulation in health and disease. *Microvasc Res* 77: 1–3, 2009.
27. **Garcia JG, Pavalko FM, Patterson CE.** Vascular endothelial cell activation and permeability responses to thrombin. *Blood Coagul Fibrinolysis* 6: 609–626, 1995.
28. **Gonzalez-Gallego J, Garcia-Mediavilla MV, Sanchez-Campos S, Tunon MJ.** Fruit polyphenols, immunity and inflammation. *Br J Nutr* 104, *Suppl* 3: S15–27, 2010.
29. **Gordon JL.** Endothelium as a modulator of platelet reactivity. *Adv Exp Med Biol* 192: 419–425, 1985.
30. **Greaves MW, Camp RD.** Prostaglandins, leukotrienes, phospholipase, platelet activating factor, and cytokines: an integrated approach to inflammation of human skin. *Arch Dermatol Res* 280: S33–41, 1988.
31. **Grega GJ.** Contractile elements in endothelial cells as potential targets for drug action. *Trends Pharmacol Sci* 7: 452–457, 1986.
32. **Grega GJ, Adamski SW.** The role of venular endothelial cells in the regulation of macromolecular permeability. *Microcirc Endothelium Lymphatics* 4: 143–167, 1988.
33. **He P.** Leucocyte/endothelium interactions and microvessel permeability: coupled or uncoupled? *Cardiovasc Res* 87: 281–290, 2010.
34. **He P, Zhang H, Zhu L, Jiang Y, Zhou X.** Leukocyte-platelet aggregate adhesion and vascular permeability in intact microvessels: role of activated endothelial cells. *Am J Physiol Heart Circ Physiol* 291: H591–H599, 2006.
35. **Hubscher SG.** Central perivenulitis: a common and potentially important finding in late posttransplant liver biopsies. *Liver Transpl* 14: 596–600, 2008.
36. **Jacobi J, Sela S, Cohen HI, Chezar J, Kristal B.** Priming of polymorphonuclear leukocytes: a culprit in the initiation of endothelial cell injury. *Am J Physiol Heart Circ Physiol* 290: H2051–H2058, 2006.
37. **Johanson CE, Stopa EG, McMillan PN.** The blood-cerebrospinal fluid barrier: structure and functional significance. *Methods Mol Biol* 686: 101–131, 2011.
38. **Juchem G, Weiss DR, Gansera B, Kemkes BM, Mueller-Hoecker J, Nees S.** Pericytes in the macrovascular intima: possible physiological and pathogenetic impact. *Am J Physiol Heart Circ Physiol* 298: H754–H770, 2010.
39. **Kim MH, Harris NR, Tarbell JM.** Regulation of hydraulic conductivity in response to sustained changes in pressure. *Am J Physiol Heart Circ Physiol* 289: H2551–H2558, 2005.
40. **Kimura M, Dietrich HH, Huxley VH, Reichner DR, Dacey RG Jr.** Measurement of hydraulic conductivity in isolated arterioles of rat brain cortex. *Am J Physiol Heart Circ Physiol* 264: H1788–H1797, 1993.
41. **Komarova Y, Malik AB.** Regulation of endothelial permeability via paracellular and transcellular transport pathways. *Annu Rev Physiol* 72: 463–493, 2010.
42. **Krieglstein CF, Granger DN.** Adhesion molecules and their role in vascular disease. *Am J Hypertens* 14: 44S–54S, 2001.
43. **Lai CH, Kuo KH, Leo JM.** Critical role of actin in modulating BBB permeability. *Brain Res Brain Res Rev* 50: 7–13, 2005.
44. **Leirisalo-Repo M.** The present knowledge of the inflammatory process and the inflammatory mediators. *Pharmacol Toxicol* 75, *Suppl* 2: 1–3, 1994.
45. **Lewandowski M.** Zur Lehre von der cerebrospinalflüssigkeit [On the cerebrospinal fluid]. *Zentralblatt Klein Forschung* 40: 480–494, 1900.
46. **Ley K.** Integration of inflammatory signals by rolling neutrophils. *Immunol Rev* 186: 8–18, 2002.
47. **Li N, Hu H, Lindqvist M, Wikstrom-Jonsson E, Goodall AH, Hjemdahl P.** Platelet-leukocyte cross talk in whole blood. *Arterioscler Thromb Vasc Biol* 20: 2702–2708, 2000.
48. **Mackman N.** Role of tissue factor in hemostasis, thrombosis, and vascular development. *Arterioscler Thromb Vasc Biol* 24: 1015–1022, 2004.
49. **Maderna P, Godson C.** Lipoxins: resolutionary road. *Br J Pharmacol* 158: 947–959, 2009.
50. **Magrone T, Jirillo E.** Polyphenols from red wine are potent modulators of innate and adaptive immune responsiveness. *Proc Nutr Soc* 69: 279–285, 2010.
51. **McDonald DM.** Endothelial gaps and permeability of venules in rat tracheas exposed to inflammatory stimuli. *Am J Physiol Lung Cell Mol Physiol* 266: L61–L83, 1994.
52. **McDonald DM, Thurston G, Baluk P.** Endothelial gaps as sites for plasma leakage in inflammation. *Microcirculation* 6: 7–22, 1999.
53. **McGee JE, Fitzpatrick FA.** Erythrocyte-neutrophil interactions: formation of leukotriene B4 by transcellular biosynthesis. *Proc Natl Acad Sci USA* 83: 1349–1353, 1986.
54. **Mehta RS.** Novel oral anticoagulants for prophylaxis and treatment of venous thromboembolism: part I (Factor Xa inhibitors). *Expert Rev Hematol* 3: 227–241, 2010.
55. **Mehta RS.** Novel oral anticoagulants. Part II: direct thrombin inhibitors. *Expert Rev Hematol* 3: 351–361, 2010.
56. **Michaux G, Cutler DF.** How to roll an endothelial cigar: the biogenesis of Weibel-Palade bodies. *Traffic* 5: 69–78, 2004.
57. **Michel T, Vanhoutte PM.** Cellular signaling and NO production. *Pflügers Arch* 459: 807–816, 2010.
58. **Middleton E Jr, Kandaswami C, Theoharides TC.** The effects of plant flavonoids on mammalian cells: implications for inflammation, heart disease, and cancer. *Pharmacol Rev* 52: 673–751, 2000.
59. **Minami T, Sugiyama A, Wu SQ, Abid R, Kodama T, Aird WC.** Thrombin and phenotypic modulation of the endothelium. *Arterioscler Thromb Vasc Biol* 24: 41–53, 2004.
60. **Nakagawa S, Deli MA, Nakao S, Honda M, Hayashi K, Nakaoke R, Kataoka Y, Niwa M.** Pericytes from brain microvessels strengthen the barrier integrity in primary cultures of rat brain endothelial cells. *Cell Mol Neurobiol* 27: 687–694, 2007.
61. **Nees S, Gerlach E, Des Rosiers C, Bock M, Becker BF, Herzog V.** [Recent knowledge about the metabolic regulation of coronary circulation, with a contribution on adenine nucleotide metabolism of coronary endothelial cells]. *Z Kardiol* 74, *Suppl* 7: 87–91, 1985.
62. **Nees S, Herzog V, Becker BF, Bock M, Des Rosiers C, Gerlach E.** The coronary endothelium: a highly active metabolic barrier for adenosine. *Basic Res Cardiol* 80: 515–529, 1985.
63. **Nees S, Juchem G, Eberhorn N, Thallmair M, Förch S, Knott M, Senftl A, Fischlein T, Reichart B, Weiss DR.** Wall structures of myocardial precapillary arterioles and postcapillary venules reexamined and reconstructed in vitro for studies on barrier functions. *Am J Physiol Heart Circ Physiol* 302: H51–H68, 2012.
64. **Nees S, Weiss DR, Senftl A, Knott M, Förch S, Schnurr M, Weyrich P, Juchem G.** Isolation, bulk cultivation, and characterization of coronary microvascular pericytes: the second most frequent myocardial cell type in vitro. *Am J Physiol Heart Circ Physiol* 302: H69–H84, 2012.
65. **Pearson JD, Gordon JL.** Nucleotide metabolism by endothelium. *Annu Rev Physiol* 47: 617–627, 1985.
66. **Powell T, Twist VW.** A rapid technique for the isolation and purification of adult cardiac muscle cells having respiratory control and a tolerance to calcium. *Biochem Biophys Res Commun* 72: 327–333, 1976.
67. **Qiao RL, Sadurski R, Bhattacharya J.** Hydraulic conductivity of ischemic pulmonary venules. *Am J Physiol Lung Cell Mol Physiol* 264: L382–L386, 1993.
68. **Rao LV, Pendurthi UR.** Regulation of tissue factor-factor VIIa expression on cell surfaces: a role for tissue factor-factor VIIa endocytosis. *Mol Cell Biochem* 253: 131–140, 2003.
69. **Raschke P, Becker BF, Leipert B, Schwartz LM, Zahler S, Gerlach E.** Postischemic dysfunction of the heart induced by small numbers of

neutrophils via formation of hypochlorous acid. *Basic Res Cardiol* 88: 321–339, 1993.
70. **Remick DG.** Interleukin-8. *Crit Care Med* 33: S466–467, 2005.
71. **Rodrigues SF, Granger DN.** Role of blood cells in ischaemia-reperfusion induced endothelial barrier failure. *Cardiovasc Res* 87: 291–299, 2010.
72. **Rose AG, Cooper DK.** Venular thrombosis is the key event in the pathogenesis of antibody-mediated cardiac rejection. *Xenotransplantation* 7: 31–41, 2000.
73. **Rumbaut RE, Wang J, Huxley VH.** Differential effects of L-NAME on rat venular hydraulic conductivity. *Am J Physiol Heart Circ Physiol* 279: H2017–H2023, 2000.
74. **Runkle EA, Antonetti DA.** The blood-retinal barrier: structure and functional significance. *Methods Mol Biol* 686: 133–148, 2011.
75. **Rybina IV, Liu H, Gor Y, Feinmark SJ.** Regulation of leukotriene A4 hydrolase activity in endothelial cells by phosphorylation. *J Biol Chem* 272: 31865–31871, 1997.
76. **Sala A, Bolla M, Zarini S, Muller-Peddinghaus R, Folco G.** Release of leukotriene A4 versus leukotriene B4 from human polymorphonuclear leukocytes. *J Biol Chem* 271: 17944–17948, 1996.
77. **Samuelsson B.** Arachidonic acid metabolism: role in inflammation. *Z Rheumatol* 50 *Suppl* 1: 3–6, 1991.
78. **Serafini M, Peluso I, Raguzzini A.** Flavonoids as anti-inflammatory agents. *Proc Nutr Soc* 69: 273–278, 2010.
79. **Serban DN, Nilius B, Vanhoutte PM.** The endothelial saga: the past, the present, the future. *Pflügers Arch* 459: 787–792, 2010.
80. **Serhan CN, Levy B.** Novel pathways and endogenous mediators in anti-inflammation and resolution. *Chem Immunol Allergy* 83: 115–145, 2003.
81. **Shapiro H, Lev S, Cohen J, Singer P.** Polyphenols in the prevention and treatment of sepsis syndromes: rationale and pre-clinical evidence. *Nutrition* 25: 981–997, 2009.
82. **Shen Q, Rigor RR, Pivetti CD, Wu MH, Yuan SY.** Myosin light chain kinase in microvascular endothelial barrier function. *Cardiovasc Res* 87: 272–280, 2010.
83. **Sies H, Schewe T, Heiss C, Kelm M.** Cocoa polyphenols and inflammatory mediators. *Am J Clin Nutr* 81: 304S–312S, 2005.
84. **Simionescu M, Simionescu N.** Ultrastructure of the microvascular wall: functional correlations. In: *Handbook of Physiology. The Cardiovascular System. Microcirculation*, edited by Renkin E, Michel C. Bethesda, MD: Am. Physiol. Soc., sect 2, vol IV, 1984, p. 41–101.
85. **Simionescu M, Simionescu N, Palade GE.** Segmental differentiations of cell junctions in the vascular endothelium. The microvasculature. *J Cell Biol* 67: 863–885, 1975.
86. **Song M, Kellum JA.** Interleukin-6. *Crit Care Med* 33: S463–465, 2005.
87. **Spite M, Serhan CN.** Novel lipid mediators promote resolution of acute inflammation: impact of aspirin and statins. *Circ Res* 107: 1170–1184, 2010.
88. **Strange C, Gottehrer A, Birmingham K, Heffner JE.** Platelets attenuate oxidant-induced permeability in endothelial monolayers: glutathione-dependent mechanisms. *J Appl Physiol* 81: 1701–1706, 1996.
89. **Tabuchi A, Kuebler WM.** Endothelium-platelet interactions in inflammatory lung disease. *Vascul Pharmacol* 49: 141–150, 2008.
90. **Totani L, Evangelista V.** Platelet-leukocyte interactions in cardiovascular disease and beyond. *Arterioscler Thromb Vasc Biol* 30: 2357–2361, 2010.
91. **Valeski JE, Baldwin AL.** Role of the actin cytoskeleton in regulating endothelial permeability in venules. *Microcirculation* 10: 411–420, 2003.
92. **van Nieuw Amerongen GP, van Hinsbergh VW.** Targets for pharmacological intervention of endothelial hyperpermeability and barrier function. *Vascul Pharmacol* 39: 257–272, 2002.
93. **Vanderhoek JY.** Role of the 15-lipoxygenase in the immune system. *Ann NY Acad Sci* 524: 240–251, 1988.
94. **Varga-Szabo D, Pleines I, Nieswandt B.** Cell adhesion mechanisms in platelets. *Arterioscler Thromb Vasc Biol* 28: 403–412, 2008.
95. **Victorino GP, Newton CR, Curran B.** Modulation of microvascular hydraulic permeability by platelet-activating factor. *J Trauma* 56: 379–384, 2004.
96. **Voisin MB, Probstl D, Nourshargh S.** Venular basement membranes ubiquitously express matrix protein low-expression regions: characterization in multiple tissues and remodeling during inflammation. *Am J Pathol* 176: 482–495, 2010.
97. **Weiss DR, Juchem G, Kemkes BM, Gansera B, Nees S.** Extensive deendothelialization and thrombogenicity in routinely prepared vein grafts for coronary bypass operations: facts and remedy. *Int J Clin Exp Med* 2: 95–113, 2009.
98. **Wittig J, Herderich M, Graefe EU, Veit M.** Identification of quercetin glucuronides in human plasma by high-performance liquid chromatography-tandem mass spectrometry. *J Chromatogr B Biomed Sci Appl* 753: 237–243, 2001.
99. **Wright B, Moraes LA, Kemp CF, Mullen W, Crozier A, Lovegrove JA, Gibbins JM.** A structural basis for the inhibition of collagen-stimulated platelet function by quercetin and structurally related flavonoids. *Br J Pharmacol* 159: 1312–1325, 2010.
100. **Wulf E, Deboben A, Bautz FA, Faulstich H, Wieland T.** Fluorescent phallotoxin, a tool for the visualization of cellular actin. *Proc Natl Acad Sci USA* 76: 4498–4502, 1979.
101. **Zarbock A, Ley K.** Mechanisms and consequences of neutrophil interaction with the endothelium. *Am J Pathol* 172: 1–7, 2008.
102. **Zarbock A, Singbartl K, Ley K.** Complete reversal of acid-induced acute lung injury by blocking of platelet-neutrophil aggregation. *J Clin Invest* 116: 3211–3219, 2006.
103. **Zhu L, He P.** fMLP-stimulated release of reactive oxygen species from adherent leukocytes increases microvessel permeability. *Am J Physiol Heart Circ Physiol* 290: H365–H372, 2006.
104. **Zimmerman GA, McIntyre TM, Prescott SM, Stafforini DM.** The platelet-activating factor signaling system and its regulators in syndromes of inflammation and thrombosis. *Crit Care Med* 30: S294–301, 2002.